NASA TECHNICAL NOTE

NASA TN D-6180

NASA TN D-6180

CLASSICAL RELAXATION OF Br_2 MOLECULES IN AN ARGON HEAT BATH

by Ronald Razner

Lewis Research Center
Cleveland, Ohio 44135

NATIONAL AERONAUTICS AND SPACE ADMINISTRATION • WASHINGTON, D. C. • FEBRUARY 1971

1. Report No.	2. Government Accession No.	3. Recipient's Catalog No.
NASA TN D-6180		

4. Title and Subtitle	5. Report Date
CLASSICAL RELAXATION OF Br_2 MOLECULES IN AN ARGON HEAT BATH	February 1971
	6. Performing Organization Code
7. Author(s)	8. Performing Organization Report No.
Ronald Razner	E-5904
9. Performing Organization Name and Address	10. Work Unit No.
Lewis Research Center National Aeronautics and Space Administration Cleveland, Ohio 44135	129-01
	11. Contract or Grant No.
12. Sponsoring Agency Name and Address	13. Type of Report and Period Covered
National Aeronautics and Space Administration Washington, D.C. 20546	Technical Note
	14. Sponsoring Agency Code

15. Supplementary Notes

16. Abstract

Classical trajectories for Br_2-Ar collisions were calculated and used to study energy transfer mechanisms for Br_2 molecules in a heat bath of Ar atoms at temperatures between 300 and 10 000 K. Probability distributions for internal energy changes and angular momentum transfers per collision were obtained by Monte Carlo averaging. At temperatures above 1000 K, coupling between vibrational and rotational motions in the Br_2 molecule was found too strong to be ignored. Implications of this and other results for studies of reaction rates and relaxation mechanisms are discussed.

17. Key Words (Suggested by Author(s))	18. Distribution Statement
Vibrational relaxation Rotational relaxation Energy transfer	Unclassified - unlimited

19. Security Classif. (of this report)	20. Security Classif. (of this page)	21. No. of Pages	22. Price*
Unclassified	Unclassified	56	$3.00

*For sale by the National Technical Information Service, Springfield, Virginia 22151

CLASSICAL RELAXATION OF BR_2 MOLECULES IN AN ARGON HEAT BATH

by Ronald Razner

Lewis Research Center

SUMMARY

Monte Carlo computer calculations of three-dimensional classical trajectories were carried out for collisions of bromine (Br_2) molecules with argon (Ar) atoms in an argon heat bath at 1800 K. Limited calculations were also performed at heat bath temperatures between 300 and 10 000 K. The results were used to study energy transfer mechanisms and to obtain probability distributions for internal energy and angular momentum changes per collision. These indicate that large changes in the internal energy of Br_2 are predominantly accompanied by large transfers in the angular momentum of the molecule. Starting with Br_2 molecules at zero angular momentum in a heat bath above 1000 K, a significant fraction of these molecules will acquire in a single collision an angular momentum large enough so that vibration-rotation coupling in the Br_2 molecule cannot be ignored. This implies that molecules with a significant vibration-rotation coupling will be common collision partners with argon atoms in successive collisions. This further implies that simple mechanisms of pure translation-vibration and pure translation-rotation energy transfer which are used in many theories of rate processes may not be adequate for the Br_2-Ar system. The relevance of these results to shock tube and other kinetic studies is discussed.

INTRODUCTION

Recent shock tube (refs. 1 to 3) and flash photolysis (refs. 4 to 6) experiments involving diatomic molecules in a heat bath of inert gas atoms have led to discussions regarding the validity of several theoretical models for chemical rate processes (refs. 1, 5, 7, and 8). The object of this work was to elucidate possible energy transfer mechanisms that may have been neglected in simplified theories of molecular relaxation. For this purpose classical three-dimensional collision trajectories were calculated for the bromine-argon (Br_2-Ar) system, and probability distributions for internal energy

changes and angular momentum transfers were evaluated. These probability distributions and also individual trajectories were studied to determine important features of such collisions. In particular, the role of angular momentum and vibration-rotation coupling in the relaxation of the bromine molecule was investigated in some detail.

The calculations were done specifically for the case of Br_2 molecules in the ground electronic state embedded in a heat bath of Ar atoms, where the population of Br_2 molecules is small enough for Br_2-Br_2 encounters to be neglected. There are three main reasons for choosing this system for investigation: (1) current interest generated by availability of extensive shock tube and flash photolysis data, (2) recent spectroscopic work on Br_2 (ref. 9) which has led to the determination of an improved ground state interaction potential (ref. 10), and (3) the fact that the ground state of Br_2 consists of a large number of closely spaced vibrational levels (ref. 11). The last feature is desirable from the standpoint of classical mechanics, where the energy levels for a molecule are taken to be continuous. Thus, one might expect that such system would provide an optimum chance for classical mechanics being relevant to the physical situation.

Throughout this report statistical tabulations of pertinent results are presented in considerable detail, since these can be of use in attempts to formulate analytical models for energy transfer processes. Unless otherwise stated, all data are presented in scaled SI units defined as follows:

Unit	Symbol	Value in SI units
Time	t	10^{-14} sec
Length	Å	10^{-10} meters
Mass	m	10^{-26} kg
Velocity	v	10^{-4} meters/sec
Energy	u	10^{-18} joules (1 joule = 10^{-7} ergs = $[6.241(97)\pm(12)]10^{18}$ eV = $[5.034(80)\pm(18)]10^{22}$ cm^{-1} = $[1.4399(8)\pm(4)]10^{20}$ kcal/mole)
Temperature	T	K
Angular momentum squared	$\lvert\vec{M}\rvert^2$ (with or without subscripts)	$m^2Å^2v^2$

COLLISION MODEL AND CALCULATION METHODS

Figure 1 shows the three-body coordinate system, where B-C represents the diatomic molecule and A the atom. The total Hamiltonian governing the three-body motion is

$$H = H_{CM} + H_{ABC}$$

where

$$H_{CM} = \frac{1}{2} m_{ABC} \left|\dot{\vec{R}}\right|^2 \tag{1}$$

$$H_{ABC} = \frac{1}{2} \mu_{BC} \left|\dot{\vec{R}}_{BC}\right|^2 + \frac{1}{2} \mu_{A,BC} \left|\dot{\vec{X}}\right|^2 + V_1\left(\left|\vec{R}_{BC}\right|\right) + V_2\left(\left|\vec{R}_{AB}\right|\right) + V_2\left(\left|\vec{R}_{AC}\right|\right) \tag{2}$$

with reduced masses given by $\mu_{BC} = m_B m_C / m_{BC}$ and $\mu_{A,BC} = m_A m_{BC} / m_{ABC}$. The H_{CM} is the kinetic energy of the A-B-C center of mass and does not contribute to the energy exchange in a collision. The vector $\vec{R}_{BC}$ locates particle B relative to particle C, while the vector $\vec{X}$ locates the atom relative to the center of mass of B-C.

The center of mass of Br_2 was taken to be the geometrical center of the molecule. Actually, a natural sample of bromine consists of ^{79}Br (50.54 percent) and ^{81}Br (49.46 percent), so that the center of mass of Br_2 corresponds to the geometrical center for only about half the molecules. It is doubtful that the error is significant here because of the large mass of Br_2 compared to mass differences between isotopic species. However, the reduced masses μ_{BC} and $\mu_{A,BC}$ were calculated from the average masses of natural samples of the elements (79.909 and 39.948 atomic mass units for Br and Ar, respectively, on the ^{12}C scale).

Interactions are taken to act along lines joining the particles and are given by

$$V_1\left(\left|\vec{R}_{BC}\right|\right) = \sum_{j=1}^{3} D_j \left\{1 - \exp\left[-\alpha_j\left(\left|\vec{R}_{BC}\right| - \left|\vec{R}_{BC}^{(e)}\right|\right)\right]\right\}^2 \tag{3}$$

$$V_2\left(\left|\vec{R}_{AB}\right|\right) = 4\epsilon\left[\left(\sigma/\left|\vec{R}_{AB}\right|\right)^{12} - \left(\sigma/\left|\vec{R}_{AB}\right|\right)^{6}\right] \tag{4}$$

$$V_2\left(\left|\vec{R}_{AC}\right|\right) = 4\epsilon\left[\left(\sigma/\left|\vec{R}_{AC}\right|\right)^{12} - \left(\sigma/\left|\vec{R}_{AC}\right|\right)^{6}\right] \tag{5}$$

Equation (3) is a potential of the form suggested in reference 12 which was fitted to an RKR potential for the Br-Br interaction by the method outlined in appendix B. Equations (4) and (5) representing the atom-molecule interaction are Lennard-Jones (6-12) potentials with constants ϵ and σ estimated from diffusion data (ref. 13) by mixing rules (private communication with Roger A. Svehla, NASA Lewis Research Center).

Hamilton's equations for the relative A-B-C motion are given by

$$\left.\begin{aligned}
\dot{\vec{R}}_{BC} &= \partial H/\partial \vec{P}_{BC} = \vec{P}_{BC}/\mu_{BC} \\
-\dot{\vec{P}}_{BC} &= \partial H/\partial \vec{R}_{BC} = \vec{i}_{BC}\partial V_1\left(\left|\vec{R}_{BC}\right|\right)/\partial\left|\vec{R}_{BC}\right| - \frac{1}{2}\vec{i}_{AB}\partial V_2\left(\left|\vec{R}_{AB}\right|\right)/\partial\left|\vec{R}_{AB}\right| \\
&\qquad + \frac{1}{2}\vec{i}_{AC}\partial V_2\left(\left|\vec{R}_{AC}\right|\right)/\partial\left|\vec{R}_{AC}\right| \\
\dot{\vec{X}} &= \partial H/\partial \vec{P} = \vec{P}/\mu_{A,BC} \\
-\dot{\vec{P}} &= \partial H/\partial \vec{X} = \vec{i}_{AB}\partial V_2\left(\left|\vec{R}_{AB}\right|\right)/\partial\left|\vec{R}_{AB}\right| + \vec{i}_{AC}\partial V_2\left(\left|\vec{R}_{AC}\right|\right)/\partial\left|\vec{R}_{AC}\right|
\end{aligned}\right\} \tag{6}$$

where $\vec{P}_{BC}$ and $\vec{P}$ are momenta conjugate to $\vec{R}_{BC}$ and $\vec{X}$, respectively, and $\vec{i}_{jk} = \vec{R}_{jk}/\left|\vec{R}_{jk}\right|$ are unit vectors. With $\epsilon = 0$ the equations would describe the motion of a free atom and a free homonuclear vibrating rotator with any vibration-rotation interaction that may be present.

For given initial conditions the equations of motion (in Cartesian coordinates) were integrated on an IBM 7094 computer usually employing a variable step-size routine developed by Dugan, Rice and Magee (ref. 14). This routine uses the principle of conservation of energy H_{ABC} to choose an optimum step-size at each time-step interval in the numerical integration. (Conservation of the square of angular momentum about the A-B-C center of mass could also be used.) One decides beforehand on a maximum variation in H_{ABC} (in this case 0.1 percent) that can be tolerated for a complete trajectory. The routine then breaks this up into step tolerances, taking large step sizes in noncritical prats of the integration, and smaller step sizes at critical parts. If after any individual step the incremental error is greater than it should be at that point, the calculation for that step is rejected and repeated with the step size halved. On the other hand, if the incremental error is smaller than the tolerance for a given step, succeeding

steps are chosen larger. In actual practice high energy conditions were more easily handled by the computer than low energy conditions (that is, a smaller portion of the allowable error was used up). Overall, this routine has proven to be much more efficient than using a fixed step size. For certain conditions to be subsequently considered, trajectories could not be calculated with sufficient accuracy by using the variable step-size routine. In such cases a small fixed time-step interval of 0.25 t was used. The correctness of the two integration methods was verified by checking time reversal invariance.

The allowed tolerance on H_{ABC} determined noise levels for the integration; that is, it established lower limits for changes in a molecule's internal energy and angular momentum. Changes larger than these lower limits could be considered significant, while changes smaller than these lower limits could be regarded as zero. By inspection of individual trajectories it was found that noise levels of 0.0001 u for energy and 0.001 $m^2 Å^2 v^2$ for angular momentum squared could be conservatively set for all trajectories studied.

An interaction radius for the atom-molecule interaction (see fig. 1) was determined empirically by calculating a series of trajectories with the atom placed initially at various distances from the B-C center of mass, and the molecule given a series of specified initial orientations. The initial translational motion of the atom was always along the vector $-\vec{X}$ for these trajectories. The initial value finally chosen for $|\vec{X}|$ was 10 Å. For larger initial values of $|\vec{X}|$ no changes in trajectories with the same initial B-C orientation could be detected above the noise level. In subsequent calculations integration was carried out from $|\vec{X}|$ = 10 Å (with $|\vec{X}|$ decreasing in time) to $|\vec{X}|$ = 10 Å (with $|\vec{X}|$ increasing in time). The latter defined final conditions for a trajectory. For each trajectory the following quantities were recorded:

(1) H_{ABC}; final, (f), and initial/final (i/f)

(2) Square of total angular momentum about A-B-C center of mass, $|\vec{M}|^2 = \vec{M} \cdot \vec{M}$ where $\vec{M} = (\vec{X} \times \vec{P}) + (\vec{R}_{BC} \times \vec{P}_{BC})$; (f) and (i/f)

(3) Impact parameter b defined as the perpendicular distance of the atom trajectory from the B-C center of mass that would result if $\epsilon = 0$

(4) $|\dot{\vec{X}}|$; (f) and (i/f)

(5) Scattering angle for atom (0 to π), $\cos^{-1}\left[\dot{\vec{X}}(i) \cdot \dot{\vec{X}}(f) / |\dot{\vec{X}}(i)| \cdot |\dot{\vec{X}}(f)|\right]$

(6) Total internal energy of B-C, $H_{BC} = \frac{1}{2}\mu_{BC}|\dot{\vec{R}}_{BC}|^2 + V_1(|\vec{R}_{BC}|)$; (f) and (i/f)

(7) Vibrational energy of B-C, $H_v = (2\mu_{BC})^{-1}(\vec{i}_{BC} \cdot \vec{P}_{BC})^2 + V_1(|\vec{R}_{BC}|)$; (f) and (i/f)

(8) Rotational energy of B-C, $H_r = |\vec{M}_{BC}|^2 / 2\mu_{BC}|\vec{R}_{BC}|^2$ where $\vec{M}_{BC} = \vec{R}_{BC} \times \vec{P}_{BC}$; (f) and (i/f)

(9) Square of angular momentum of B-C, $|\vec{M}_{BC}|^2 = \vec{M}_{BC} \cdot \vec{M}_{BC}$; (f) and (i/f)

(10) Kinetic energy of relative motion, $H_A = \frac{1}{2}\mu_{A,BC}|\dot{\vec{X}}|^2$; (f) and (i/f)

(11) Angle between initial and final B-C angular momentum vectors when $|\vec{M}_{BC}|^2(i) \neq 0$, $\cos^{-1}\left[\vec{M}_{BC}(i) \cdot \vec{M}_{BC}(f)/|\vec{M}_{BC}(i)| \cdot |\vec{M}_{BC}(f)|\right]$

Initial conditions were either assigned values or else were randomly selected from an appropriate distribution function by means of the formulas derived in appendix C. The molecule was assigned an initial energy H_{BC} and also a magnitude for its angular momentum vector. The orientation of the angular momentum vector and the orientation of the molecule were then randomly distributed over a sphere. Internal energy and angular momentum were given assigned initial values in preference to vibrational energy H_v and rotational energy H_r because the former are constants of the motion for the free molecule, while the latter are not.

With the atom initially at a distance of 10 Å from the center of mass of the molecule (see fig. 1), the magnitude of the relative momentum $|\vec{P}|$ was chosen from a Maxwell-Boltzmann flux distribution corresponding to a specified heat bath temperature T, while the orientation of this momentum was randomly distributed over a half sphere. The impact parameter b was calculated from the initial conditions and compared to a preassigned maximum impact parameter b_{max}. When $b \leq b_{max}$ the trajectory was calculated and the collision termed a real collision (RCOL). When $b > b_{max}$ the trajectory was not calculated and the collision was called a null collision (NCOL). These latter cases, although not calculated, were nevertheless counted as events for the determination of the distributions for energy and angular momentum changes in a collision.

The maximum impact parameter was calculated as $b_{max} = \frac{1}{2}\left|\vec{R}_{BC}\right|_{max} + 2^{1/6}\sigma$, where $\left|\vec{R}_{BC}\right|_{max}$ is the outer classical turning point in the B-C vibration and the second term locates the minimum in the Br-Br interaction. This choice of b_{max} was made because trajectories with $b > b_{max}$ were found, by trial, not to contribute significantly to the overall energy transfer.

A statistical sample of initial atom energies $H_A(i)$ must be distributed as a Maxwell-Boltzmann flux distribution (ref. 15)

$$dw = \left(\frac{H_A}{kT}\right)\exp\left(\frac{-H_A}{kT}\right)\left(\frac{dH_A}{kT}\right)$$

for RCOL alone, for NCOL alone, and for RCOL and NCOL taken together. Table I shows how well this was accomplished for a typical set of data consisting of 5229 total collisions, of which 1756 were RCOL (corresponding to the row labeled $H_{BC}(i)/D_e = 0.5$, $|\vec{M}_{BC}|^2(i) = 0$ in table III).

In scaled units the physical constants relevant to this report are as follows (with $i = (-1)^{1/2}$):

$$k = 0.138054\times10^{-4}\ uK^{-1}$$

$$\hbar^2 = 0.111197\times10^{-3}\ u^2t^2$$

$$D_1 = 0.31801\ u$$

$$D_2 = 0.57547\times10^{-3} - i0.88651\times10^{-3}\ u$$

$$D_3 = 0.57547\times10^{-3} + i0.88651\times10^{-3}\ u$$

$$\alpha_1 = 0.19756\times10^{1}\ A^{-1}$$

$$\alpha_2 = 0.15994\times10^{1} + i0.64990\times10^{1}\ Å^{-1}$$

$$\alpha_3 = 0.15994\times10^{1} - i0.64990\times10^{1}\ Å^{-1}$$

$$\left(\sum_1^3 D_j\right) = D_e = 0.31916\ u$$

$$\sigma = 0.3867\times10^{1}\ Å$$

$$\epsilon = 0.3411\times10^{-2}\ u$$

$$|\vec{R}_{BC}(e)| = 0.228161\times10^{1}\ Å$$

$$\mu_{BC} = 0.663420\times10^{1}\ m$$

$$\mu_{A,BC} = 0.530667\times10^{1}\ m$$

VIBRATION-ROTATION COUPLING IN THE FREE Br_2 MOLECULE

As observed in the preceding section, the rotational energy H_r and vibrational energy H_v are not constants of the motion for the free diatomic molecule, whereas the internal energy $H_{BC} = H_v + H_r$ is a constant of the motion. This is due to the fact that H_r is proportional to $1/|\vec{R}_{BC}|^2$, which varies with the vibrational motion. As a result, whenever the molecule possesses a finite angular momentum, a periodic coupling between H_v and H_r exists in phase with the vibrational motion. Thus, as a preliminary step to considering atom-molecule collisions, the amplitude of vibration-rotation coupling was calculated for a range of internal energies and angular momenta and compared to quantum mechanical vibrational level spacings (J = 0) obtained from RKR calculations (see appendix B). It is likely that the phenomenon of vibration-rotation coupling, shown schematically in figure 2, may become significant for an atom-diatomic collision theory whenever the coupling amplitude in the free molecule is comparable to energy spacings in successive RKR levels.

For a measure of the H_v, H_r coupling we can use the peak-to-peak amplitude of vibrational energy $H_v(p - p)$ defined by

$$H_v(p - p) = H_{v,\,max} - H_{v,\,min}$$

where $H_{v,\,max}$ is the instantaneous vibrational energy corresponding to the outer classical turning point in the B-C vibration, and $H_{v,\,min}$ corresponds to the inner classical turning point. This amplitude was determined at constant H_{BC} as a function of $|\vec{M}_{BC}|^2$ for the free Br_2 molecule from dummy trajectories obtained by setting $\epsilon = 0$ in the equations of motion and conserving H_{BC} to a tolerance of 0.05 percent. The results are shown in figure 3 for $H_{BC} = 0.1\ D_e$, $0.5\ D_e$, and $0.9\ D_e$. (The curve labeled $H_{BC,\,max}$ in fig. 3 is considered separately at the end of this section.) One point together with its coordinates is shown on each curve. From $|\vec{M}_{BC}|^2 = 0$ up to this point $H_v(p - p)/H_{BC}$ increases linearly with increasing $|\vec{M}_{BC}|^2$ to within the limits set by the noise level in the integration.

A list of RKR (J = 0) vibrational levels (see appendix B) for the ground state of the $^{79}Br^{81}Br$ molecule is given in table II. Using this table together with figure 3, one can determine the extent of H_v, H_r coupling and can estimate when a theory of energy transfer conceived as a process of transitions between pure vibrational levels is likely to fail. For example, a coupling amplitude of $H_v(p - p)/H_{BC} = 0.01$ corresponds approximately to 1/20 of a RKR vibrational level spacing at $H_{BC} = 0.1\ D_e$, 1/3 of a level spacing at $0.5\ D_e$, and 1 level spacing at $0.9\ D_e$.

Average values for H_v and H_r were also determined for the free molecule (at constant H_{BC}) as a function of $|\vec{M}_{BC}|^2$ by integrating the vibration and rotation energy functions according to the relation

$$\langle H_{v,r} \rangle = \left(\frac{1}{t}\right) \int_0^t H_{v,r}\, dt \tag{7}$$

At constant H_{BC},

$$\langle H_v \rangle = H_{BC} - \left(|\vec{M}_{BC}|^2 / 2\mu_{BC} \right) \left\langle 1/|\vec{R}_{BC}|^2 \right\rangle \tag{8}$$

where $\left\langle |\vec{R}_{BC}|^2 \right\rangle$ is the mean square of the internuclear separation. To a good approximation the numerical data can be expressed by a linear relation:

$$\langle H_v \rangle = H_{BC} - x|\vec{M}_{BC}|^2 \tag{9}$$

where $x = 0.0143$ at $H_{BC} = 0.1\, D_e$, $x = 0.0134$ at $H_{BC} = 0.5\, D_e$, and $x = 0.0084$ at $H_{BC} = 0.9\, D_e$ (with energies and angular momentum expressed in scaled units). Corresponding constant values of $\left\langle |\vec{R}_{BC}|^2 \right\rangle$ are 5.27(1), 5.62(5), and 8.9(7) Å^2, respectively. (Uncertain figures are enclosed in parenthesis.) The linear relation holds for $H_{BC} = 0.1\, D_e$ and $0.5\, D_e$ as far as the calculations were taken (up to $|\vec{M}_{BC}|^2 = 10$ or $H_v = 0$), whereas for $H_{BC} = 0.9\, D_e$ the linear relation is valid up to $|\vec{M}_{BC}|^2 = 1.0$. For larger angular momenta at $H_{BC} = 0.9\, D_e$ the numerical value of x increases slowly to 0.01 and then varies irregularly between $0.0099 \lesssim x \lesssim 0.0130$ with increasing $|\vec{M}_{BC}|^2$. This increase of x with $|\vec{M}_{BC}|^2$ reflects the fact that at constant H_{BC} an increase of $|\vec{M}_{BC}|^2$ produces an increase in H_r, and hence a decrease in H_v. The smaller H_v, however, implies a smaller $\left\langle |\vec{R}_{BC}|^2 \right\rangle$. The irregularities in x at large $|\vec{M}_{BC}|^2$ are perhaps an indication that some errors are being accumulated in the integration of the equations of motion at high rotational energies. However, in all cases the average rotational and vibrational energies satisfy $H_{BC} = \langle H_v \rangle + \langle H_r \rangle$.

Also shown in figure 3 is a H_v, H_r coupling curve for the molecule near dissociation, which for present purposes is defined to be $H_{v,\max} \geq 0.9999\, D_e$. (It is not practical to define dissociation as $H_{v,\max} \geq D_e$ because the condition $|\vec{R}_{BC}| \to \infty$ cannot be handled by the computer.) With this definition the maximum internal energy $H_{BC,\max}$ that the molecule can have without dissociating is determined from dummy trajectories to be

$$H_{BC,\max}/D_e < 0.9999 + y|\vec{M}_{BC}|^2 \tag{10}$$

where energies and angular momentum squared are expressed in scaled units and $y = 0.0100 \pm 0.0001(m^2 \mathring{A}^2 v^2)^{-1}$. The H_v, H_r coupling curve for $H_{BC,\max}$ is almost linear, in contrast to the other curves in figure 3, because the former was calculated for constant $H_{v,\max}$ instead of for constant H_{BC}.

SIGNIFICANT FEATURES OF INDIVIDUAL Br_2-Ar COLLISIONS

A typical atom-molecule trajectory for close encounters is shown in figure 4, where energies and distances are plotted as functions of time. (This particular example was taken from data with initial conditions $H_{BC}(i) = 0.1\ D_e$, $|\vec{M}_{BC}|^2(i) = 0$, and $T = 1800$ K.) Most of the energy transfer occurred within a small time interval, comparable in magnitude to the time required for one cycle in the Br_2 vibration. In terms of the atom-molecule interaction this time interval corresponds to Br-Ar distances where V_2 becomes repulsive. (One cannot conclude from this that the attractive terms in V_2 may be ignored. The statistical influence of these terms is considered later in this report.) Also evident in the figure is the existence of a significant H_v, H_r coupling, which was discussed in the preceding section. In this section the influence of atom velocity on impulsive collisions and the sensitivity of trajectories to changes in poetntial constants are considered.

Dependence of Impulsive Collisions on Initial Atom Energy

Many simple atom-diatomic collision theories make use of an impulsive collision approximation, where atom-to-molecule energy transfer is considered to take place in the duration of one molecular vibration period or less. For the present collision model we have investigated whether a collision that is impulsive at high heat bath temperatures would remain impulsive as the heat bath temperature is lowered. For this purpose a series of trajectories with identical impact parameters and Br_2 initial conditions was calculated by scaling the components of initial atom velocity, $\dot{X}_1$, $\dot{X}_2$, $\dot{X}_3$ (see appendix C) for the trajectory in figure 4 to correspond to heat bath temperatures from 300 to 10 000 K where

$$\dot{X}_j(T) = (T/1800)^{1/2}\, \dot{X}_j(1800) \tag{11}$$

Results are shown for T = 300, 1000, 1800, and 10 000 K in figures 5(a) to (d), respectively, where the variables $|\vec{R}_{BC}|$, H_{BC}, and H_r are plotted the same way as in figure 4. Since the initial frequency of the B-C vibration (as indicated by $|\vec{R}_{BC}|$) is the same in all these figures, one sees that if a collision is impulsive at $T > 1000$ K, it will likely remain impulsive as the atom velocity is decreased to correspond to a heat bath temperature as low as 300 K. However, there are limitations to this statement that are considered in the concluding discussion of this report.

Sensitivity of Trajectories to Potential Constants

An attempt was made to estimate the sensitivity of individual trajectories to changes in potential constants by recalculating the trajectory shown in figure 4 under the following conditions: (1) use of a simple Morse potential instead of equation (3) where $D_1 = D_e$, $D_2 = D_3 = 0$, $\alpha_1 = 0.19689 \times 10^{1}$ Å^{-1}; (2) $\epsilon = 0.2411 \times 10^{-2}$ u; (3) $\epsilon = 0.4411 \times 10^{-21}$ u; (4) $\sigma = 0.4367 \times 10^{1}$ Å; and (5) $\sigma = 0.3367 \times 10^{1}$ Å. In each case, all constants not listed had the original values. These changes in the atom-molecule interaction V_2 are probably more drastic than any changes that could be expected from improved experimental data. For example, even for other inert gases we estimate the constants: $\epsilon = 0.995 \times 10^{-3}$ u, $\sigma = 0.3438 \times 10^{1}$ Å for He; $\epsilon = 0.1878 \times 10^{-2}$ u, $\sigma = 0.3544 \times 10^{1}$ Å for Ne; $\epsilon = 0.4072 \times 10^{-2}$ u, $\sigma = 0.3984 \times 10^{1}$ Å for Kr; $\epsilon = 0.4597 \times 10^{-2}$ u, $\sigma = 0.4180 \times 10^{1}$ Å for Xe; and almost all of these lie within the previous variations in ϵ and σ. Final values and the ratio (i/f) are listed for all pertinent quantities - first for the original trajectory in figure 4 then for cases (1) to (5):

Impact parameter: same for all trajectories; b = 0.2338711 Å

Scattering angle (radians): 2.6092621, (1) 2.6104993, (2) 2.6244507, (3) 2.5905407, (4) 2.6970121, (5) 2.4579556

H_{ABC}(i): same for all trajectories; H_{ABC}(f) = 0.09076595 u (original)

H_{ABC}(i/f): 1.0000893, (1) 1.0001728, (2) 1.0001322, (3) 1.0001293, (4) 1.0001100, (5) 1.0002308

H_{BC}(i/f): 0.5682207, (1) 0.5626052, (2) 0.5719623, (3) 0.5632753, (4) 0.6167731, (5) 0.5173918

H_A(i): same for all trajectories; H_A(f) = 0.03459789 u (original)

H_A(i/f): 1.7012077, (1) 1.7501041, (2) 1.6830058, (3) 1.7265491, (4) 1.5097518, (5) 2.0231369

$|\vec{M}_{BC}|^2$(f): 1.6896222 m^{2}Å^{2}v, (1) 1.6551220, (2) 1.5350854, (3) 1.8447367, (4) 1.7241471, (5) 1.7011569

The use of the Morse potential resulted in displacing both the original maximum (0.0357 u) and minimum (0.0286 u) in the final H_v upward by 0.0019 u.

In this report, the concern is mainly with the total energy transferred to the molecule ΔH_{BC} and also the angular momentum transfer $\Delta|\vec{M}_{BC}|^2$. These are considered in the next section. To significantly alter any statistical results to be discussed, ΔH_{BC} and $\Delta|\vec{M}_{BC}|^2$ revisions due to changes in potential constants of at least a half order of magnitude for individual trajectories would have to add up in a noncompensating way for a major portion of the real collisions (RCOL) involved in a random sampling. I believe it is safe to say that any such revision is extremely unlikely, and hence that the constants ϵ and σ are adequately determined for present purposes.

Estimate of Three-Body Interactions

The interactions (3) to (5) chosen for the present collision model assume only a pairwise additivity of forces acting along lines joining particles A, B, and C. In dense systems such as compressed gases, liquids, and solids, pairwise interactions may no longer be adequate, and a consideration of three-body and many-body forces might then be necessary. Hence, the question may arise as to what influence a three-body potential term, $V_3\left(|\vec{R}_{AB}|, |\vec{R}_{BC}|, |\vec{R}_{AC}|\right)$, would have on individual trajectories.

To estimate the possible influence of three-body forces a potential of the form of a van der Waals interaction between three atoms was used (ref. 16):

$$V_3 = \frac{\nu}{\left(|\vec{R}_{AB}| \cdot |\vec{R}_{BC}| \cdot |\vec{R}_{AC}|\right)^3} (1 + 3 \cos A \cos B \cos C) \qquad (12)$$

where cos A, cos B, and cos C are cosines of the angles BAC, ABC, and ACB, respectively, and the constant ν was assumed to have the value $\nu = 7.32\ u\text{Å}^9$ which holds for Ar-Ar-Ar interactions (ref. 17). For the trajectory in figure 4, V_3 came to within 0.1 percent of the total energy ($0.001\ H_{ABC}$) for only a few time units during the closest approach of the atom to the molecule. At the same time, however, the interaction V_2 was more than 150 times that of V_3. Consequently, it appears that if the value used for ν is at least of the correct order of magnitude, then no significant error will result by completely neglecting three-body forces.

CALCULATIONS FOR Br_2 MOLECULES IN AN ARGON HEAT BATH

Probability Distributions for ΔH_{BC} and $\Delta|\vec{M}_{BC}|^2$

Probability distributions for the molecule undergoing a change ΔH_{BC}, $\Delta|\vec{M}_{BC}|^2$ per collision with an argon atom randomly selected from the heat bath were determined for given initial values of internal energy $H_{BC}(i)$ and angular momentum squared $|\vec{M}_{BC}|^2(i)$. A family of such distributions is illustrated schematically in figure 6. Each distribution curve depends on all the initial conditions

$$f(\Delta H_{BC}) = f\left(\Delta H_{BC};\ H_{BC}(i),\ |\vec{M}_{BC}|^2(i),\ T\right)$$

$$f\left(\Delta|\vec{M}_{BC}|^2\right) = f\left(\Delta|\vec{M}_{BC}|^2;\ H_{BC}(i),\ |\vec{M}_{BC}|^2(i),\ T\right)$$

so that each set of initial conditions $\left(H_{BC}(i),\ |\vec{M}_{BC}|^2(i),\ T\right)$ determines a specific distribution for ΔH_{BC} and a specific distribution for $\Delta|\vec{M}_{BC}|^2$. From a data set consisting of 5229 total collisions, of which 1756 were RCOL, calculated for initial conditions (0.5 D_e, 0, 1800 K), it was found that data sets consisting of 1000 RCOL were sufficient to determine any given distribution. For an initial angular momentum $|\vec{M}_{BC}|^2(i) = 0$, the distribution $f\left(\Delta|\vec{M}_{BC}|^2\right)$ would consist of only a "gains" branch. A statistical equilibrium for ΔH_{BC} or $\Delta|\vec{M}_{BC}|^2$ would result if "gains" and "losses" branches for the corresponding distributions were symmetric, whereas a relaxation would occur if either a "gains" or a "losses" branch were predominant. Several types of equilibrium conditions which are relevant to subsequent discussions can be defined as follows, where n stands for noise level:

(1) Overall gains-losses balance for ΔH_{BC}

$$\int_{-\infty}^{-n} f(\Delta H_{BC})d(\Delta H_{BC}) = \int_{+n}^{+\infty} f(\Delta H_{BC})d(\Delta H_{BC}) \tag{13}$$

(2) Overall gains-losses balance for $\Delta|\vec{M}_{BC}|^2$

$$\int_{-\infty}^{-n} f\left(\Delta|\vec{M}_{BC}|^2\right)d\left(\Delta|\vec{M}_{BC}|^2\right) = \int_{+n}^{+\infty} f\left(\Delta|\vec{M}_{BC}|^2\right)d\left(\Delta|\vec{M}_{BC}|^2\right) \tag{14}$$

(3) Simultaneous gains-losses balance for ΔH_{BC} and $\Delta|\vec{M}_{BC}|^2$ when conditions (1) and (2) are both satisfied

(4) Statistical equilibrium for ΔH_{BC} (gains and losses branches symmetric)

$$\int_{-\infty}^{-a} f(\Delta H_{BC})d(\Delta H_{BC}) = \int_{+a}^{+\infty} f(\Delta H_{BC})d(\Delta H_{BC}) \quad \text{for all } a \geq n \tag{15}$$

(5) Statistical equilibrium for $\Delta|\vec{M}_{BC}|^2$

$$\int_{-\infty}^{-a} f\left(\Delta|\vec{M}_{BC}|^2\right)d\left(\Delta|\vec{M}_{BC}|^2\right) = \int_{+a}^{+\infty} f\left(\Delta|\vec{M}_{BC}|^2\right)d\left(\Delta|\vec{M}_{BC}|^2\right) \quad \text{for all } a \geq n \tag{16}$$

(6) Simultaneous statistical equilibruium for ΔH_{BC} and $\Delta|\vec{M}_{BC}|^2$ when conditions (4) and (5) are both satisfied

Tables III and IV list probability distributions for several combinations of initial conditions in terms of the fraction of total trajectories resulting in changes in a given ΔH_{BC} or $\Delta|\vec{M}_{BC}|^2$ range. From these tables several results are apparent. For most initial conditions, a major portion of the total trajectories is within the noise level of the calculation, and relatively few trajectories are responsible for the bulk of the energy and angular momentum transfer. Referring to table III as an example, one finds that collisions of the latter type are distributed so that, with $|\vec{M}_{BC}|^2(i) = 0$ and $H_{BC}(i)$ from 0 to 0.9 D_e, after a single collision 28 to 38 percent of the molecules have $|\vec{M}_{BC}|^2 \geq 0.001$, 23 to 29 percent $|\vec{M}_{BC}|^2 \geq 0.01$, 17 to 21 percent $|\vec{M}_{BC}|^2 \geq 0.1$, and 4 to 9 percent $|\vec{M}_{BC}|^2 \geq 1.0$. In terms of the quantum formula $|\vec{M}_{BC}|^2 = \hbar^2 J(J+1)$ these correspond (to the nearest integer) to transitions from $J = 0$ to $J \geq 3$, 9, 30, and 95, respectively.

It should be emphasized that all fractional populations in tables III and IV are given on a total collision basis. These would change if the radius of the sphere of interaction were changed, because increasing the radius of the sphere of interaction would increase the proportion of NCOL. On the other hand, the relative distribution of RCOL in given ΔH_{BC} and $\Delta|\vec{M}_{BC}|^2$ ranges does not depend on the radius of interaction provided this is chosen large enough so that the atom and molecule can be considered initially free. By using the ratios of real collisions to total collisions in the tables, the fractional populations as given can be converted to a RCOL basis. Thus, for example, if 5.8 percent of the molecules with $H_{BC}(i) = 0.5\ D_e$ and $|\vec{M}_{BC}|^2(i) = 0$ at $T = 1800$ K have $|\vec{M}_{BC}|^2 \geq 1.0$ after a single collision, this represents 17.3 percent of the real collisions.

Calculations where the internal energy of the molecule H_{BC} is close to the dissociation energy D_e present a special problem in that the molecule can dissociate during a trajectory. Thus, final conditions for such trajectories must be defined as $|\vec{X}| = 10$ A with $|\vec{X}|$ increasing in time, or $H_v \geq 0.9999\ D_e$, whichever occurs first (see eq. (10)). Trajectories of this type were calculated for T = 1800 K, and the resulting probability distributions are included in table III. For each initial angular momentum $|\vec{M}_{BC}|^2(i)$, initial energies were set at $H_{BC}(i) = 0.999\ H_{BC,\,max}$ (see eq. (10)), and trajectories were calculated using a constant time-step size to avoid false dissociations by accumulation of integration errors. For these calculations b_{max} was set at 7.966 Å, which corresponds to $2^{1/6}\sigma + \frac{1}{2}\left|\vec{R}_{BC}\right|_{max}$ for $H_{v,\,max} = 0.9999\ D_e$. This value of b_{max} was found by trial to include all those trajectories capable of supplying the small increment of energy needed for dissociation. From table III it is seen that the probability of a molecule dissociating increases significantly as $|\vec{M}_{BC}|^2(i)$ increases from zero. The nature of angular momentum changes in the dissociation process is shown in figure 7, which compares the frequency of events where dissociation proceeds with an increase in $|\vec{M}_{BC}|^2$, with the frequency of dissociations accompained by a decrease in $|\vec{M}_{BC}|^2$. The table in the figure shows the noise level population of dissociation events. For small initial angular momenta dissociation events with a gain in angular momentum outnumber dissociation events with a loss in angular momentum. As $|M_{BC}|^2(i)$ increases the loss-to-gain ratio for dissociation events reaches a maximum, and then decreases.

Sensitivity of ΔH_{BC} and $\Delta|\vec{M}_{BC}|^2$ Distributions to Heat Bath Temperature

When the results in table IV are plotted, the behaviors of ΔH_{BC} and $\Delta|\vec{M}_{BC}|^2$ probability distributions as functions of heat bath temperature can be obtained for initial conditions $\left(H_{BC}(i), |M_{BC}|^2(i)\right) = (0, 0)$, $(0.5\ D_e, 0)$, and $(0.5\ D_e, 1.0)$. Such plots are shown in figures 8(a) and (b). It appears that distributions over a wide range of heat bath temperatures can be obtained with reasonable confidence by interpolation once calculations have been done for a few temperatures. It is also seen that for ΔH_{BC} and $\Delta|\vec{M}_{BC}|^2$ ranges which include small to intermediate changes, there is a significant difference in the temperature dependence of probability distributions, depending on whether or not the molecule has an initial angular momentum. The most pronounced differences are in the heat bath temperature range of 300 to 2000 K. In this region ΔH_{BC} and $\Delta|\vec{M}_{BC}|^2$ gains for initial conditions (0, 0) and $(0.5\ D_e, 0)$ are decreasing functions of temperature, while those for $(0.5\ D_e, 1.0)$ are increasing functions of temperature. The opposite dependence is found for ΔH_{BC} losses for $(0.5\ D_e, 0)$ and $(0.5\ D_e, 1.0)$. Thus, in the temperature range of greatest interest (corresponding to

most of the available experimental data) it would appear that a consideration of angular momentum transfers as well as internal energy changes is important.

Relation Between ΔH_{BC} and $\Delta|\vec{M}_{BC}|^2$ Distributions

For given initial conditions the probability distributions $f(\Delta H_{BC})$ and $f\left(\Delta|\vec{M}_{BC}|^2\right)$ are not independent of each other; that is, given a specific energy change ΔH_{BC}, all $\Delta|\vec{M}_{BC}|^2$ changes in the distribution $f\left(\Delta|\vec{M}_{BC}|^2\right)$ are not allowed and vice versa. The correspondence between internal energy and angular momentum changes was determined for each data set in tables III and IV. Results are presented as gain-loss matrices in tables V, VI, and VII, where entries represent fractions of RCOL (including changes within the noise level).

Table V correlates overall gains and losses for T = 1800 K, where it is seen that diagonal changes $\left(\Delta H_{BC}, \Delta|\vec{M}_{BC}|^2\right)$ = (g, g) and (ℓ, ℓ) are the most probable. Much less probable are off-diagonal changes, the least probable being those in the (g, ℓ) quadrant (with the possible exception of conditions near dissociation which are complicated by dissociation events). Diagonal events appear to undergo a smooth transition with increasing $|\vec{M}_{BC}|^2$(i) from a dominance in the (g, g) quadrant to a dominance in the (ℓ, ℓ) quadrant. Also, as $|\vec{M}_{BC}|^2$(i) increases from zero, events in the (ℓ, g) quadrant appear to undergo a steady decrease (conditions near dissociation excluded). However, the least probable off-diagonal quadrant (g, ℓ) behaves differently from the other three in that its population first increases with increasing $|\vec{M}_{BC}|^2$(i), reaches a maximum, and then decreases. Finally, with the possible exception of conditions near dissociation, an equilibrium or balance in diagonal events does not coincide with a balance in off-diagonal events. The latter, if it occurs (not certain with present calculations), occurs at a higher $|\vec{M}_{BC}|^2$(i) than the balance for diagonal events.

Table VI consists of a breakdown of each quadrant in the matrices of table V into subquadrants which separate large changes from small changes. Table VII is a similar compilation for the data sets in table IV. The dividing line for energy was set at ΔH_{BC} = 0.01 u, which is about three times the zero point energy. (Vibrational transitions from RKR level 0 to RKR levels 1 and 2 would correspond to ΔH_v = 0.0054 u and 0.0127 u, respectively.) Internal energy changes less than this were arbitrarily called small, and those at or above 0.01 u were called large. Similarly, the dividing line for $\Delta|\vec{M}_{BC}|^2$ was set at 0.1 $m^2 Å^2 v^2$ (or J = 30). Partitions labeled 1 correspond to small energy and small angular momentum changes; those labeled 2 correspond to small energy and large angular momentum changes; those labeled 3 correspond to large energy and small angular momentum changes; and those labeled 4 correspond to large energy and large angular momentum changes. Partitions 1 include all those changes which

correspond to $|\Delta q| \lesssim 1$ for H_v, where q is the RKR vibrational quantum number, whereas partitions 3 would include all pure (or almost pure) vibrational energy changes where $|\Delta q| \gtrsim 2$. For all conditions it is seen that the probability of the latter is almost negligible. Of all RCOL, the most probable changes are large and small energy gains (losses) accompained by significant angular momentum gains (losses), as represented by the sum of partitions 2_{gg} and 4_{gg} for angular momentum gains and the sum of partitions 2_{ll} and 4_{ll} for angular momentum losses.

Equilibrium as a Function of Heat Bath Temperature

Sets of initial conditions, $\left(H_{BC}(i), |\vec{M}_{BC}|^2(i), T\right)$, were determined which result in overall gains-losses balances for ΔH_{BC} and/or $\Delta|\vec{M}_{BC}|^2$ by graphically locating solutions to equations (13) and (14) which define these balances. Results are presented in table VIII for $H_{BC}(i) = 0.5\ D_e$ through a heat bath temperature range of 300 to 10 000 K, and for $H_{BC}(i) = 0.1\ D_e$ and $0.9\ D_e$ at a heat bath temperature of 1800 K. Also given in table VIII is a comparison of the vibrating-rotator balance points with mean angular momenta for rigid rotators at various internuclear spacings according to equilibrium statistical mechanics. Since $|\vec{R}_{BC}|^2$ for a rigid rotator is constant, the mean internal energy is simply $\frac{1}{2}$ kT per degree of freedom, or $\langle H_r \rangle = kT = \left\langle |\vec{M}_{BC}|^2 \right\rangle / 2\mu_{BC}|\vec{R}_{BC}|^2$. From this table it appears that if one were given initial conditions $H_{BC}(i)$ and T for the vibrating-rotator and wished to estimate a corresponding value of $|\vec{M}_{BC}|^2(i)$ that would result in a $\Delta|\vec{M}_{BC}|^2$ balance, the required estimate for $T \leq 1800$ K would correspond moderately well to $\left\langle |\vec{M}_{BC}|^2 \right\rangle$ for a rigid rotator with an internuclear spacing equal to the average internuclear spacing for the vibrating-rotator at the given energy. (See discussion accompanying eq. (9).) For example, a $\Delta|\vec{M}_{BC}|^2$ balance occurs at $|\vec{M}_{BC}|^2(i) = 0.98$ for the vibrating rotator with $H_{BC}(i) = 0.5\ D_e$ and T = 1000 K. The corresponding $\left\langle |\vec{M}_{BC}|^2 \right\rangle$ for the rigid rotator is 1.03, a difference of only 5 percent. However, as the temperature increases beyond 1800 K, the vibrating rotator balance occurs at angular momenta corresponding to a rigid rotator with decreasing internuclear spacing. At T = 10 000 K this spacing is approximately equal to the inner classical turning point for the vibrating rotator.

Whereas the equilibrium angular momentum for a rigid rotator is simply a constant times the heat bath temperature, one finds that for the vibrating rotator a plot of values of $|\vec{M}_{BC}|^2(i)$, which yield $\Delta|\vec{M}_{BC}|^2$ balances as functions of heat bath temperature, has a curvature that becomes more pronounced as the heat bath temperature increases. If at constant $H_{BC}(i)$ a similar plot is constructed for values of $|\vec{M}_{BC}|^2(i)$ corresponding to ΔH_{BC} balances, the ΔH_{BC} and $\Delta|\vec{M}_{BC}|^2$ curves intersect at a heat bath temperature corresponding to a simultaneous gains-losses balance for ΔH_{BC} and

$\Delta|\vec{M}_{BC}|^2$. Interestingly enough, this temperature corresponds approximately to a statistical equilibrium temperature for internal energy obtained by setting $H_{BC}(i) = \frac{3}{2}kT$.

Investigations similar to the previous one could perhaps be carried out for internal energies near dissociation, but here the situation is complicated by the fact that molecules are dissociating with a probability of dissociation that depends on $|\vec{M}_{BC}|^2(i)$. Calculations performed so far are not extensive enough to consider such conditions further in this report.

The information presented in this and preceding sections permits an estimate of the magnitude of H_v, H_r coupling likely to exist in the Br_2 molecule as it collides with an Ar atom. Even if a collection of molecules with zero initial angular momentum were embedded in a heat bath at $T > 1000$ K, after a few collisions a considerable fraction of these molecules would possess angular momenta of the order $|\vec{M}_{BC}|^2 > 1$. If the angular momenta corresponding to gains-losses balances in table VIII are regarded as typical for Br_2 molecules under the specified conditions, then from figure 3 it is seen that a H_v, H_r coupling amplitude of the order of 10 percent or more of H_{BC} would be common. At internal energies $H_{BC} \gtrsim 0.5\, D_e$ this corresponds to a coupling amplitude well in excess of the RKR vibrational level spacing.

Scattering Angle and Reorientation of $\vec{M}_{BC}$

The atom scattering angle and also the angle between the initial and final B-C angular momentum vectors (for $|\vec{M}_{BC}|^2 \neq 0$) were tabulated and studied. Unfortunately I did not decide to record the latter quantity until this work was well under way, and hence results cannot be given for all data sets in tables III and IV. However, sufficient results are included for a meaningful study of trends.

For all data sets, the scattering angle populations decreased monotonically with increasing scattering angle. As might be expected, the decrease was most rapid at the highest heat bath temperatures, showing that atom trajectories for high energy collisions are effectively straight lines.

For planar motion (two-dimensional theories) the $\vec{M}_{BC}$ reorientation angle would be restricted to the values 0 or π, whereas in the present three-dimensional collision model this angle can have any value in the interval $[0, \pi]$. Tabulations of the $\vec{M}_{BC}$ reorientation angle together with ΔH_{BC} and $\Delta|\vec{M}_{BC}|^2$ indicate that a large angle almost always implies large energy and angular momentum changes. Events consisting of a large reorientation of the $\vec{M}_{BC}$ vector with little or no net change in H_{BC} and $|\vec{M}_{BC}|^2$ were extremely rare.

The way in which the $\vec{M}_{BC}$ reorientation angle populations were distributed (for RCOL) is shown by bar graphs in figure 9 for all data sets where this quantity was recorded. Each bar graph indicates the angle intervals representing approximately 50, 70, and 90 percent of the data. (The exact fractions as tabulated are given above each bar graph, since tabulations were only performed for steps of 0.1 radian.) Some trends are discernible for data taken at fixed $H_{BC}(i)$ and $|\vec{M}_{BC}|^2(i)$ through a range of temperatures and at fixed $H_{BC}(i)$ and temperature through a range of $|\vec{M}_{BC}|^2(i)$. Data for (0.5 D_e, 1.0, T) show a slight increase in the range of $\vec{M}_{BC}$ reorientation angles with increasing temperature up to 3000 K, but a restriction to angles of 0.1 radian or less at 10 000 K. This restriction to small angles at 10 000 K holds for all angular momenta that were considered, except for a sharp increase for the data set (0.5 D_e, 8.24, 10000 K), which is a gains-losses balance point for $\Delta|\vec{M}_{BC}|^2$. This may indicate the possibility of a resonance at gains-losses balance conditions, where the probability of large $\vec{M}_{BC}$ reorientation angles increases. Such possibility for ΔH_{BC} and/or $\Delta|\vec{M}_{BC}|^2$ balance conditions is suggested by comparing the data sets (0.5 D_e, 0.25, 300 K), (0.5 D_e, 0.82, 1000 K), (0.5 D_e, 1.48, 1800 K), and (0.9 D_e, 2.0, 1800 K) with others in figure 9. Finally, the data sets near dissociation at 1800 K show a decrease in the range of $\vec{M}_{BC}$ reorientation angles as the angular momentum increases. (The three bar graphs in fig. 9 labeled "attractive term in V_2 removed" are discussed below.)

Plots of scattering angle as a function of the $\vec{M}_{BC}$ reorientation angle showed a random scatter of data points, and hence no apparent statistical correlation between these two quantities.

Effect of Removing the Attractive Part of V_2

Some theories neglect the attractive term in a potential of the form V_2. Hence, I have evaluated the effect of the attractive terms by removing $-(\sigma/|\vec{R}_{AB}|)^6$ and $-(\sigma/|\vec{R}_{AC}|)^6$ from the atom-molecule interaction and recalculating three probability distributions - (0.5 D_e, 0.25, 300 K), (0.5 D_e, 1.48, 1800 K) and (0.5 D_e, 8.24, 10 000 K). Results are presented in table IX in the form of probability distributions and in the form of matrix tabulations as previously discussed. Since ϵ/k = 247 K, one might expect the greatest influence to be for heat bath temperatures close to this value. A comparison of table IX with corresponding entries in tables IV and VII confirms this expectation. In particular, the calculations at 300 K show almost a perfect gains-losses balance for $\Delta|M_{BC}|^2$, in contrast to a predominance in gains for calculations with the attractive V_2 terms included. At 1800 K what was previously a gains-losses balance for ΔH_{BC} is now converted to a dominance in losses. Results for 10 000 K

are unchanged. Finally, figure 9 includes tabulations for the $\vec{M}_{BC}$ reorientation angle, which again shows a large influence of the attractive interaction at 300 K.

RESULTS AND DISCUSSION

Diatomic molecule-third body collision theories of energy transfer are often conceived in terms of translation-rotation processes (rotational relaxation) and translation-vibration processes (vibrational relaxation) where the two pure transfer modes are assumed to be independent to a good approximation. (A recent review of vibrational and rotational relaxation processes is given in ref. 18.) The former process is characteristic of rigid rotator theories, and the latter process of collinear collision models. Most of the theories of dissociation of diatomics involve in some way the idea of exciting an unperturbed oscillator, such as the quantum mechanical process of vibrational ladder climbing, with an activation energy for dissociation equated to the dissociation energy. However, attempts to correlate theory with experiment (ref. 1) have indicated that an activation energy is probably less than the dissociation energy. This being the case, energy transfer mechanisms other than a pure translation-vibration process must be sought.

From an inspection of individual trajectories (e.g., see fig. 5) we have concluded that one may, to a good approximation, assume an impulsive energy transfer between the atom and the diatomic molecule. Such an assumption is common to many theories and has been used, for example, in the quantum mechanical calculations of Bak and Fisher (ref. 19). However, this does not necessarily mean that such impulsive energy transfer can be construed as a pure vibrational or pure rotational excitation. Rather, it appears that a sizeable portion of the trajectories responsible for the bulk of the energy transfer (RCOL) will involve molecules with a significant vibration-rotation coupling, commonly exceeding one or more RKR vibrational level spacings. As a consequence, the molecules would be so perturbed that one could not justify considering a dissociation process in terms of a pure translation-vibration energy exchange. For example, it has been pointed out by Bak and Fisher (ref. 19) that if activation and dissociation energies are not equal, one could not assume a random walk on the energy levels of an unperturbed oscillator. At best the process would have to be considered as a H_A to H_{BC} transfer with vibrational and rotational modes in the B-C motion cross-feeding each other. Dissociation would presumably have to be defined as $H_{v,\max} \geq D_e$, but at a given average vibrational energy $\langle H_v \rangle$ sufficient angular momentum could be added to the molecule to make it dissociate at the outer classical turning point in the vibrational motion. In addition, a comparison of the way probability distributions for $|\vec{M}_{BC}|^2(i) = 0$ and $|\vec{M}_{BC}|^2(i) \gg 0$ vary with heat bath temperature indicates signifi-

cant differences. Hence, it would not be surprising for theories that ignore the influence of angular momentum to yield significantly different dissociation rates, compared to theories that include the effect of angular momentum. Any discrepancies between various theories should increase as the average number of collisions per dissociation event increases, because each collision is effectively a change ΔH_{BC}, $\Delta|\vec{M}_{BC}|^2$ which is governed by distributions $f(\Delta H_{BC})$ and $f\left(\Delta|\vec{M}_{BC}|^2\right)$.

Lewis Research Center,
National Aeronautics and Space Administration,
Cleveland, Ohio, October 9, 1970,
129-01.

APPENDIX A

SYMBOLS

$\mathring{A}$	scaled unit of length, 10^{-10} meters
c	speed of light
D_e	dissociation energy for Br_2
D_j	potential constants for Br - Br intraction, $\sum D_j = D_e$
H	Hamiltonian (total energy)
H_A	kinetic energy of relative Br_2-Ar motion
H_{ABC}	energy of relative motion of particles A, B, and C
H_{BC}	internal energy of Br_2
H_{CM}	kinetic energy of translation of Br_2-Ar center of mass
H_r	rotational energy
H_v	vibrational energy
$\hbar^2$	Planck's constant squared divided by $4\pi^2$
$\vec{i}_{ij}$	unit vector
J	rotational quantum number
k	Boltzmann's constant
$\vec{M}$	angular momentum about A-B-C center of mass
$\vec{M}_{BC}$	angular momentum about Br_2 center of mass
m	scaled unit of mass, 10^{-26} kg, subscripts indicate masses of particles
$\vec{P}$	relative Br_2-Ar momentum
$\vec{P}_{BC}$	momentum of particle B relative to particle C
q	vibrational quantum number
$\vec{R}_{BC}$	location of particle B relative to particle C
$\lvert\vec{R}_{BC}(e)\rvert$	equilibrium internuclear separation for Br_2
T	temperature,
t	scaled unit of time, 10^{-14} sec
u	scaled unit of energy, 10^{-18} joules

$V(x)$	interaction potential
$V_1(\|\vec{R}_{BC}\|)$	interaction potential for Br-Br
$V_2(\|\vec{R}_{AB}\|), V_2(\|\vec{R}_{AC}\|)$	atom-molecule interaction potentials
$V_3(\|\vec{R}_{AB}\|, \|\vec{R}_{BC}\|, \|\vec{R}_{AC}\|)$	three-body potential
v	scaled unit of velocity, 10^4 m/sec
$\vec{X}$	location of Ar relative to Br_2 center of mass
Z	symbol for a random number in the interval $[0,1]$ (with or without subscripts)
α_j	potential constants in Br-Br interaction, V_1
α_M	potential constant in Morse potential
ϵ	Lennard-Jones potential constant in V_2
Θ	longitude in cylindrical coordinates
θ	colatitude in spherical polar coordinates
μ	reduced mass (with or without subscripts)
σ	Lennard-Jones potential constant in V_2
ν	potential constant for V_3
φ	longitude in spherical polar coordinates
$\left.\begin{matrix}\omega_o, \omega_o x_o, \omega_o y_o, \omega_e \\ \omega_e x_e, \omega_e y_e, \omega_e z_e\end{matrix}\right\}$	molecular constants

APPENDIX B

CURVE FITTING PROCEDURE FOR $V_1(|\vec{R}_{BC}|)$

The potential $V_1(|\vec{R}_{BC}|)$ (see eq. (3)) is the generalization of the Morse function

$$V_M(x) = D_e\left(1 - e^{-\alpha_M x}\right)^2 \tag{B1}$$

suggested in reference 12 that can be made to coincide with "true" RKR potential calculations for diatomic molecules to a degree not possible with a simple Morse function. This generalized potential is of the form of a sum of three Morse functions

$$V(x) = \sum_1^3 D_j\left(1 - e^{-\alpha_j x}\right)^2 \tag{B2}$$

where $x = |\vec{R}_{BC}| - |\vec{R}_{BC}(e)|$ and $D_e = \sum D_j$ is the dissociation energy referred to V(0). In equation (B2) pairs of D_j and pairs of α_j may occur as complex conjugates, with the restriction $\mathrm{Re}(\alpha_j) > 0$ to ensure that the potential remains finite as $x \to \infty$.

In attempting to construct a potential of the form of equation (B2) we have found that literally following the procedure given in reference 12 will not unequivocally lead to physically acceptable solutions. For $^{79,81}Br_2$ both older (ref. 9) and recently revised molecular constants (ref. 10) led to complex α_j with negative real parts. The situation was not changed for $^{79,79}Br_2$ and $^{81,81}Br_2$ where molecular constants were estimated from the isotope effect (ref. 11). However, given RKR calculations, one can replace the first part of the calculation in reference 12 with a direct method of curve fitting. This yields a similar set of final equations for the D_j and α_j where certain numerical criteria established in reference 12 (to be explained) are not required. Using the spectroscopic constants of LeRoy and Burns (ref. 10), we have determined V(x) corresponding to the ground state of $^{79,81}Br_2$. The RKR potential was first recalculated with a program available at this laboratory (ref. 20). The value of D_e (16068 cm^{-1}) was obtained from the experimental value for D_o of 15906 cm^{-1} (ref. 9) plus the zero point energy of 162 cm^{-1}. Our calculations agree closely with those in reference 10, except in the following particulars. There is a very slight discrepancy in that a calculation of spectroscopic energy as a function of vibrational quantum number (for J = 0) using the constants given in reference 10 possesses a maximum at 16053.7 cm^{-1}, which is in-

consistent with the dissociation energy of 16068 cm^{-1}. Our RKR calculations give 78 vibrational levels up to the energy 16053.7 cm^{-1} (see table II) instead of the 80 levels reported by LeRoy and Burns. Also we find $|\bar{R}_{BC}(e)| = 2.28161$ Å compared to LeRoy and Burns' value of 2.2814 Å.

Let $V(x_q)$ be the potential energy at a given RKR level q and $F_j(x_q) = \left(1 - e^{-\alpha_j x_q}\right)^2$. Then

$$D_1F_1(x_q) + D_2F_2(x_q) + D_3F_3(x_q) = V(x_q) \tag{B3}$$

where $F_j(x_q)$ can be expanded as

$$F_j(x_q) = \sum_{n=2}^{\infty} \left[(2^n - 2)/n!\right]\left(-\alpha_j x_q\right)^n \tag{B4}$$

Substituting (B4) into (B3) and retaining terms up to x_q^6 gives

$$D_1\left[\left(-\alpha_1 x_q\right)^2 + \left(-\alpha_1 x_q\right)^3 + (7/12)\left(-\alpha_1 x_q\right)^4 + (1/4)\left(-\alpha_1 x_q\right)^5 + (62/720)\left(-\alpha_1 x_q\right)^6\right]$$

$$+ D_2\left[\left(-\alpha_2 x_q\right)^2 + ---\right] + D_3\left[\left(-\alpha_3 x_q\right)^2 + ---\right] \approx V(x_q) \tag{B5}$$

Defining $G_k \equiv D_1\alpha_1^k + D_2\alpha_2^k + D_3\alpha_3^k$, with $k = 0, 2, 3, 4, 5, 6$, $G_0 = D_e$, and the other G_k obtained from RKR data, equation (B5) becomes

$$\left(x_q\right)^2 G_2 - \left(x_q\right)^3 G_3 + (7/12)\left(x_q\right)^4 G_4 - (1/4)\left(x_q\right)^5 G_5 + (62/720)\left(x_q\right)^6 G_6 = V(x_q) \tag{B6}$$

where $\approx$ has been replaced by $=$ for the purpose of curve fitting. Five values of x_q (for classical turning points) and corresponding values of $V(x_q)$ are now chosen so as to be representative of the RKR calculations over the range of energies for which an accurate curve fit is desired. This gives five equations which are then treated as simultaneous equations and solved for numerical values of G_2 to G_6. These values of G_k plus G_0 are then used to determine the D_j and α_j from solutions to the dimensionless equations:

$$b_k = \sum_{J=1}^{3} \varkappa_j \gamma_j^k \qquad (k = 0, 2, 3, 4, 5, 6) \tag{B7}$$

where $b_0 = 1$, $b_k = G_k/D_e\alpha_M^k$, $\varkappa_j = D_j/D_e$, and $\psi_j = \alpha_j/\alpha_M$. These equations are solved for $\varkappa_j$ and ψ_j by the method suggested in reference 12. The value of α_M is calculated from

$$\alpha_M = (\omega_o + \omega_o x_o)\left(\pi c \mu/\hbar D_e\right)^{1/2} \tag{B8}$$

where c is the speed of light and μ the reduced mass.

In the calculations of reference 12, equation (B8) is the first step in an iterative procedure for $\alpha(\neq\alpha_M)$ from $\omega_o + \omega_o x_o + p\omega_o y_o = \alpha\left(\hbar D_e/\pi c\mu\right)^{1/2}$ where p is an iteration parameter and neglecting $p\omega_o y_o$ gives $\alpha = \alpha_M$. For the case of Br_2 the iteration converges with the initial step for a considerable numerical range of p. This may be a source of difficulty. The quantities ω_o, $\omega_o x_o$, $\omega_o y_o$ are calculated from the molecular constants ω_e, $\omega_e x_e$, $\omega_e y_e$, $\omega_e z_e$ by

$$\omega_o = \omega_e - \omega_e x_e + (3/4)\omega_e y_e + (1/2)\omega_e z_e$$

$$\omega_o x_o = \omega_e x_e - (3/2)\omega_e y_e - (3/2)\omega_e z_e$$

$$\omega_o y_o = \omega_e y_e + 2\omega_e z_e$$

For $^{79,81}Br_2$ we have (in cm^{-1}), $\omega_e = 324.24$, $\omega_e x_e = 1.172$, $\omega_e y_e = 0.00342$, and $\omega_e z_e = -0.000101$ (ref. 10).

For present purposes we have chosen two RKR points for $|\vec{R}_{BC}| < |\vec{R}_{BC}(e)|$ and three points for $|\vec{R}_{BC}| > |\vec{R}_{BC}(e)|$ $(q = 18_-, 2_-, 0_+, 4_+, 18_+)$ for which values of b_k were determined as

$$b_0 = 1 \qquad b_4 = 0.6743075$$

$$b_2 = 0.9960699 \qquad b_5 = 3.441186$$

$$b_3 = 0.7493079 \qquad b_6 = 8.840423$$

In general there will be two sets of solutions for $\varkappa_j$ and ψ_j, but in the present instance only one set was physically acceptable. In the procedure of reference 12 $b_0 = b_2 = 1$ always, $b_3^2 = b_4$, and b_5 and b_6 are sought as close to unity as possible, such criterion being in principle necessary for convergence in these authors' original expansion. In our case we obtain values for b_2, b_3, and b_4 close to those obtained by the method of reference 12 (although $b_3^2 \neq b_4$); but, values for b_5 and b_6 considerably exceed

unity. The D_j and α_j corresponding to these b_k are given in the text (see p. 7). The potential so determined was found to be a significant improvement over the Morse potential for low vibrational energies, but no improvement above $q = 18$. This curve fit was a compromise between a desire to achieve as close a fit as possible for low lying RKR vibrational levels and a desire to represent the required curvature on both sides of $|\vec{R}_{BC}(e)|$ for high vibrational levels. By fitting the potential to more points for any desired portion of the RKR calculations one can, of course, achieve a better fit for that portion. For example, choosing $q = 10_-, 0_+, 3_+, 5_+, 10_+$ resulted in a fit for $|\vec{R}_{BC}| > |\vec{R}_{BC}(e)|$ to within 1 percent of the RKR calculations up to $q = 60$, but a poor fit for $|\vec{R}_{BC}| < |\vec{R}_{BC}(e)|$.

APPENDIX C

SELECTION OF INITIAL CONDITIONS

In this appendix the relations used in selecting initial conditions for the atom and molecule are derived. Present calculations involve collisions between molecules with specified internal energies and atoms selected at random from a heat bath. Consequently, initial conditions for the molecule involve only a random orientation of position and velocity vectors over a sphere, while initial conditions for the atom in the present collision model must be selected from a probability distribution corresponding to a Maxwell-Boltzmann flux distribution for the atoms at the specified heat bath temperature. (The general method for choosing initial conditions from a known distribution is given in ref. 21.) Implicit in the latter is the assumption that the translational temperatures of the molecules and atoms are the same. This situation corresponds to the common assumption in shock tube work that translational temperatures of all species are equalized in the shocked gas, while the internal degrees of freedom for molecules are in the process of "relaxing" toward equilibrium.

Initial Conditions for the Atom

An atom selected from the Maxwell-Boltzmann flux distribution with temperature T is placed on the surface of a sphere centered at the center of mass of the molecule, and with a radius equal to the interaction radius for the atom-molecule interaction (10 Å). Without loss of generality the initial position was set at $X_1 = X_2 = 0$, $X_3 = -10$ Å (see fig. 1). Initial atom velocities were then chosen at random from

$$N \exp(-H_A/kT) d\dot{\vec{X}} \tag{C1}$$

where N is a normalization factor to be determined. The flux distribution of atoms across the $X_1 - X_2$ plane is

$$f d\dot{\vec{X}} = N \vec{i}_3 \cdot \dot{\vec{X}} \exp\left(-\frac{1}{2} \beta \mu_{A,BC} \left|\dot{\vec{X}}\right|^2\right) d\dot{\vec{X}} \tag{C2}$$

where $\beta = 1/kT$ and $\vec{i}_3$ is a unit vector along the X_3 axis. One must determine N such that $\int f d\dot{\vec{X}} = 1 = \left\langle \vec{i}_3 \cdot \dot{\vec{X}} \right\rangle$ where $\left\langle \vec{i}_3 \cdot \dot{\vec{X}} \right\rangle$ is the average over the Maxwell-Boltzman flux distribution for $\dot{\vec{X}}$:

$$f d\dot{\vec{X}} = \left(\vec{i}_3 \cdot \dot{\vec{X}} / \langle \vec{i}_3 \cdot \dot{\vec{X}} \rangle\right) \exp\left(-\frac{1}{2}\beta\mu_{A,BC}\left|\dot{\vec{X}}\right|^2\right) d\dot{\vec{X}} \tag{C3}$$

We introduce cylindrical coordinates for $\dot{\vec{X}}$ by

$$\left.\begin{aligned} \dot{X}_1 &= \left|\dot{\vec{X}}\right| \cos\Theta \\ \dot{X}_2 &= \left|\dot{\vec{X}}\right| \sin\Theta \\ \dot{X}_3 &= \vec{i}_3 \cdot \dot{\vec{X}} \end{aligned}\right\} \tag{C4}$$

The distribution f is then

$$\dot{X}_3 \exp\left[-\frac{1}{2}\beta\mu_{A,BC}\left(\left|\dot{\vec{X}}\right|^2 + \dot{X}_3^2\right)\right]\left|\dot{\vec{X}}\right| d\left|\dot{\vec{X}}\right| d\Theta\, d\dot{X}_3 = \left[\exp\left(-\frac{1}{2}\beta\mu_{A,BC}\left|\dot{\vec{X}}\right|^2\right)\left|\dot{\vec{X}}\right| d\left|\dot{\vec{X}}\right|\right] \times \left[\exp\left(-\frac{1}{2}\beta\mu_{A,BC}\dot{X}_3^2\right)\dot{X}_3\, d\dot{X}_3\right](d\Theta) \tag{C5}$$

where $\left|\dot{\vec{X}}\right|$ goes from 0 to ∞. Letting $\left|\dot{\vec{X}}\right|^2 = s$ and $a = \frac{1}{2}\beta\mu_{A,BC}$ gives

$$\frac{1}{2}\int_0^\infty \exp(-as)ds = 1/2a \tag{C6}$$

so that the normalized integral is

$$2a\int_0^\infty \exp\left(-a\left|\dot{\vec{X}}\right|^2\right)\left|\dot{\vec{X}}\right| d\left|\dot{\vec{X}}\right| = 1$$

Also,

$$\frac{1}{2}\int_0^s \exp(-as)ds = -(1/2a)\exp(-as)\Big]_0^s = (1/2a)\left(1 - \exp\left(-a\left|\dot{\vec{X}}\right|^2\right)\right) \tag{C7}$$

Thus the normalized $\dot{\vec{X}}$ distribution is

$$\left[(1/\beta\mu_{A,BC})\exp\left(-\frac{1}{2}\beta\mu_{A,BC}\left|\dot{\vec{X}}\right|^2\right)\left|\dot{\vec{X}}\right| d\left|\dot{\vec{X}}\right|\right]\left[(1/\beta\mu_{A,BC})\exp\left(-\frac{1}{2}\beta\mu_{A,BC}\dot{X}_3^2\right)\dot{X}_3\, d\dot{X}_3\right]$$

$$\times [d\Theta/2\pi] \qquad \text{(C8)}$$

while the cumulative distributions are

$$\left.\begin{aligned} Z'_{1,2} &= 1 - \exp\left(-\frac{1}{2}\beta\mu_{A,BC}\left|\dot{\vec{X}}\right|^2\right) \\ Z'_3 &= 1 - \exp\left(-\frac{1}{2}\beta\mu_{A,BC}\dot{X}_3^2\right) \\ Z'_\Theta &= \Theta/2\pi \end{aligned}\right\} \qquad \text{(C9)}$$

Setting the cumulative distribution functions (C9) equal to random numbers in the interval $[0, 1]$ and recognizing that one minus a random number is also a random number in $[0, 1]$ gives

$$\left.\begin{aligned} \Theta &= 2\pi Z_\Theta \\ \left|\dot{\vec{X}}\right| &= \left(-2\ln Z_{1,2}/\beta\mu_{A,BC}\right)^{1/2} \\ \dot{X}_3 &= \left(-2\ln Z_3/\beta\mu_{A,BC}\right)^{1/2} \end{aligned}\right\} \qquad \text{(C10)}$$

where Z_Θ, $Z_{1,2}$, and Z_3 are random numbers. Thus, the initial conditions from (C4) become

$$\left.\begin{aligned} \dot{X}_1 &= \left(-2\ln Z_{1,2}/\beta\mu_{A,BC}\right)^{1/2}\cos(2\pi Z_\Theta) \\ \dot{X}_2 &= \left(-2\ln Z_{1,2}/\beta\mu_{A,BC}\right)^{1/2}\sin(2\pi Z_\Theta) \\ \dot{X}_3 &= \left(-2\ln Z_3/\beta\mu_{A,BC}\right)^{1/2} \end{aligned}\right\} \qquad \text{(C11)}$$

Initial conditions are generated by selecting random numbers $Z_{1,2}$, Z_3, and Z_Θ from a linear distribution in the interval [0, 1] and substituting into equation (C11). If this is repeated many times, initial kinetic energies $H_A(i)$ will be distributed according to a Maxwell-Boltzmann flux distribution at temperature T, as shown in table I.

Initial Conditions for the Molecule, Given H_{BC} and $|\vec{M}_{BC}|^2$

The orientation of $\vec{R}_{BC}$ must be randomly distributed over a sphere. Thus, introducing the spherical polar coordinates

$$\left.\begin{aligned} R_{BC,1} &= |\vec{R}_{BC}| \sin\theta \cos\varphi \\ R_{BC,2} &= |\vec{R}_{BC}| \sin\theta \sin\varphi \\ R_{BC,3} &= |\vec{R}_{BC}| \cos\theta \end{aligned}\right\} \tag{C12}$$

and choosing $|\vec{R}_{BC}|(i) = |\vec{R}_{BC}(e)|$, we have

$$\left.\begin{aligned} \varphi &= 2\pi Z_\varphi \\ \theta &= \cos^{-1}(1 - 2Z_\theta) \end{aligned}\right\} \tag{C13}$$

where Z_φ and Z_θ are random numbers in the interval [0, 1].

One can choose $|\vec{R}_{BC}|(i)$ anywhere between $|\vec{R}_{BC}|_{max}$ and $|\vec{R}_{BC}|_{min}$ provided the $|\vec{R}_{BC}|$ distribution function can be integrated in closed form. If this cannot be done, approximations to the distribution must be made. Originally our program specified H_v and H_r and chose $|\vec{R}_{BC}|(i)$ from a linear distribution between $|\vec{R}_{BC}|_{min}$ and $|\vec{R}_{BC}|_{max}$. However tabulation of results for $|\vec{M}_{BC}|^2(i) = 0$ trajectoris indicated no detectable difference from tabulations where $|\vec{R}_{BC}|(i) = |\vec{R}_{BC}(e)|$. In general, the molecule underwent several complete vibrations before the atom came close enough to cause significant energy transfer, and it appears that statistical results are not sensitive to the choice of $|\vec{R}_{BC}|(i)$.

For velocity components of the molecule, equation (C12) is differentiated with respect to time, and with $V_1(|\vec{R}_{BC}|)(i) = 0$, $|\dot{\vec{R}}_{BC}|(i)$ is calculated from $\frac{1}{2}\mu_{BC}|\dot{\vec{R}}_{BC}|^2 = H_v$

where $H_v = H_{BC} - H_r$. A ± sign is then affixed to the result (by random number selection) with equal probability of either choice. A plane of rotation is selected by choosing

$$|\dot{\theta}| = |\dot{\Phi}|Z \tag{C14}$$

where Z is a random number and $|\dot{\Phi}| = \left(2 H_r/\mu_{BC}|\vec{R}_{BC}(e)|^2\right)^{1/2}$ is the magnitude of the instaneous angular velocity in the plane of rotation, and a ± sign is randomly affixed to $|\dot{\theta}|$. Finally $|\dot{\varphi}|$ is calculated from

$$|\vec{M}_{BC}|^2/\mu_{BC}^2 = |\vec{R}_{BC}(e)|^4\dot{\Phi}^2 = |\vec{R}_{BC}(e)|^4(\dot{\varphi}^2\sin^2\theta + \dot{\theta}^2)$$

or

$$\dot{\varphi}^2 = (\dot{\Phi}^2 - \dot{\theta}^2)/\sin^2\theta \tag{C15}$$

and a ± sign is randomly affixed to the result. With the initial components for $\vec{R}_{BC}$ and $\dot{\vec{R}}_{BC}$ thus chosen, the computer then calculates H_{BC} and $|\vec{M}_{BC}|^2$ and compares the results with the actual input before proceeding with the integration. In the unlikely event that $|\dot{\theta}| = 0$ or $|\dot{\Phi}|$, and/or $\theta = 0$ or π, the computer rechooses θ, φ, and $\dot{\theta}$.

REFERENCES

1. Warshay, Marvin: Shock - Tube Investigation of Bromine Dissociation Rates in Presence of Argon, Neon, and Krypton. NASA TN D-3502, 1966.

2. Boyd, R. K.; Burns, George; Lawrence, T. R.; and Lippiatt, J. H.: Dissociation and Two - Body Emission in Shock - Heated Bromine. I. Br_2 in Argon. J. Chem. Phys., vol. 49, no. 9, Nov. 1, 1968, pp. 3804-3821.

3. Warshay, Marvin: Effects of Boundary Layer Buildup in Shock Tubes upon Chemical Rate Measurements. NASA TN D-4795, 1968.

4. Ip, J. K. K.; and Burns, George: Recombination of Br Atoms by Flash Photolysis over a Wide Temperature Range. Disc. Faraday Soc., no. 44, Molecular Dynamics of the Chemical Reactions of Gases, 1967, pp. 241-251.

5. General Discussion. Disc. Faraday Soc., no. 44, Molecular Dynamics of the Chemical Reactions of Gases, 1967, pp. 273-285.

6. Ip, J. K. K.; and Burns, George: Recombination of Br Atoms by Flash Photolysis over a Wide Temperature Range. II. Br_2 in He, Ne, Ar, Kr, N_2, O_2. J. Chem. Phys., vol. 51, no. 8, Oct. 15, 1969, pp. 3414-3424.

7. Berend, George C.; and Benson, Sidney W.: Vibrational Relaxation Times of Br_2 in Ar. J. Chem. Phys., vol. 48, no. 10, May 15, 1968, pp. 4793-4794.

8. Ip, J. K. K.; and Burns, George: Negative Temperature Coefficient of Atomic Recombination Rate Constants from Flash Photolysis and Shock - Wave Data. Bromine. J. Chem. Phys., vol. 51, no. 8, Oct. 15, 1969, pp. 3425-3433.

9. Rao, Yerneni Venkateswara; and Venkateswarlu, Putcha: Vacuum Ultraviolet Resonance Spectrum of Br_2 Molecule. J. Mol. Spectros., vol. 13, no. 3, July, 1964, pp. 288-295.

10. LeRoy, Robert J.; and Burns, George: A Method for Testing and Improving Molecular Constants of Diatomic Molecules with Special Reference to Br_2 $^1(\sum_g^+)$. J. Mol. Spectros., vol. 25, no. 1, Jan., 1968, pp. 77-85.

11. Herzberg, Gerhard: Spectra of Diatomic Molecules. Second ed. vol. 1, of Molecular Structure. Van Nostrand-Reinhold, 1950, p. 456.

12. Flügge, S.; Walger, P; and Weiguny, A.: A Generalization of the Morse Potential for Diatomic Molecules. J. Mol. Spectros., vol. 23, no. 3, July, 1967, pp. 243-257.

13. Rabinowitch, E.; and Wood, W. C.: The Heterogeneous Recombination and the Diffusion Coefficients of Halogen Atoms. Trans. Faraday Soc., vol. 32, 1936, pp. 917-922.

14. Dugan, John V. Jr.; Rice, James H.; and Magee, John L.: Calculation of Capture Cross Sections for Ion - Polar - Molecule Collisions Involving Methyl Cyanide. NASA TM X-1586, 1968, App. B.

15. Zeleznik, Frank J.: Rotational Relaxation in Polar Gases. J. Chem. Phys., vol. 47, no. 9, Nov. 1, 1967, pp. 3410-3424, Eq. (18).

16. Axilrod, B. M.; and Teller, E.: Interaction of the Van der Waals Type Between Three Atoms. J. Chem. Phys., vol. 11, no. 6, June, 1943, pp. 299-300.

17. Barker, J. A.; Henderson, D.; and Smith, W. R.: Pair and Triplet Interactions in Argon. Molec. Phys., vol. 17, no. 6, Dec. 1969, pp. 579-592.

18. Gordon, Roy G.; Klemperer, William; and Steinfeld, Jeffrey I.: Vibrational and Rotational Relaxation. Ann. Rev. of Phys. Chem., vol. 19, 1968, pp. 215-250.

19. Bak, Thor A.; and Fisher, Edward R.: The Relaxation and Dissociation of Small Molecules. AGARD Conference Proceedings No. 12, Recent Advances in Aerothermochemistry, vol. 1, Glassman, ed., 1967, pp. 47-57.

20. Zeleznik, Frank J.: Numerical Calculation of Potential - Energy Curves by the Rydberg - Klein - Rees Method. J. Chem. Phys., vol. 42, no. 8, April 15, 1965, pp. 2836-2838.

21. Goldstein, Charles M.: Monte Carlo Method for the Calculation of Transport Properties in a Low - Density Ionized Gas. NASA TN D-2959, 1965, App. A.

TABLE I. - FRACTIONAL POPULATIONS OF INITIAL ATOM ENERGIES FOR T = 1800 K

u	$\left[\left(\sum_{H=u}^{\infty}\text{RCOL}\right)/\sum\text{RCOL}\right]_A$	$\left[\left(\sum_{H=u}^{\infty}\text{NCOL}\right)/\sum\text{NCOL}\right]_A$	$\left[\left(\sum_{H=u}^{\infty}(\text{RCOL}+\text{NCOL})\right)/\sum(\text{RCOL}+\text{NCOL})\right]_A$	Required population $\int_u^{\infty} dw$
0	1	1	1	1
.01	.9476	.9359	.9398	.9378
.02	.8126	.8065	.8086	.8071
.03	.6538	.6616	.6589	.6600
.04	.5102	.5302	.5240	.5218
.05	.4043	.4184	.4137	.4027
.06	.3058	.3234	.3175	.3053
.07	.2341	.2426	.2397	.2282
.08	.1731	.1759	.1749	.1687
.09	.1310	.1268	.1282	.1236
.10	.1002	.0918	.0947	.0898

TABLE II. - RKR(J = 0) VIBRATIONAL ENERGY LEVELS

FOR $^{79}Br\ ^{81}Br$ GROUND STATE ($^1\Sigma_g^+$)

Vibrational quantum number, q	$H_v \div D_e$	Vibrational quantum number, q	$H_v \div D_e$
0	0.01007	40	0.69485
1	.03011	41	.70839
2	.05000	42	.72170
3	.06974	43	.73479
4	.08935	44	.74764
5	.10881	45	.76026
6	.12813	46	.77263
7	.14731	47	.78476
8	.16635	48	.79662
9	.18525	49	.80823
10	.20401	50	.81957
11	.22263	51	.83063
12	.24111	52	.84142
13	.25944	53	.85191
14	.27763	54	.86212
15	.29568	55	.87202
16	.31359	56	.88162
17	.33135	57	.89090
18	.34896	58	.89986
19	.36643	59	.90849
20	.38375	60	.91679
21	.40091	61	.92474
22	.41792	62	.93233
23	.43478	63	.93957
24	.45147	64	.94643
25	.46801	65	.95292
26	.48439	66	.95903
27	.50060	67	.96474
28	.51664	68	.97004
29	.53252	69	.97494
30	.54821	70	.97941
31	.56374	71	.98345
32	.57908	72	.98705
33	.59423	73	.99020
34	.60920	74	.99289
35	.62398	75	.99512
36	.63856	76	.99686
37	.65294	77	.99811
38	.66712	78	.99886
39	.68109		

TABLE III. - PROBABILITY DISTRIBUTIONS FOR ΔH_{BC} AND $\Delta|\vec{M}_{BC}|^2$ PER COLLISION AT T = 1800 K

[Entry n means given interval is within noise level; all entries except $H_{BC}(i) = 0.5\ D_e$, $|\vec{M}_{BC}|^2(i) = 0$ are based on 1000 RCOL; exception contains 1756 RCOL; estimate of reliability for fractional populations is ±0.01.]

$\frac{H_{BC}(i)}{D_e}$ | $|\vec{M}_{BC}|^2(i)$ | $\frac{\sum(RCOL)}{\sum(RCOL + NCOL)}$ | Fraction of (RCOL + NCOL) dissociated | $w_1 = \int_f^y f(\Delta H_{BC})d(\Delta H_{BC})$ | $w_2 = \int_x^y f\left(\Delta|\vec{M}_{BC}|^2\right)d\left(\Delta|\vec{M}_{BC}|^2\right)$

w_1/w_2

				Integral lower limit, x										
				-∞	-∞	-∞	-∞	-∞	-∞	-n	0.0001	0.001	0.01	0.1	1.0
				Integral upper limit, y											
				∞	-1.0	-0.1	-0.01	-0.001	-0.0001	n	∞	∞	∞	∞	∞
0	0	[a]0.308	0	1/1	0/0	0/0	0/0	0/0	0/0	0.760/0.721	0.240/n	0.189/0.279	0.062/0.233	0/0.173	0/0.042
0.1	0	0.318	0	1/1	0/0	0/0	0.000/0	0.005/0	0.015/0	0.758/0.713	0.227/n	0.176/0.287	0.062/0.234	0.001/0.171	0/0.046
0.1	0.01	0.315	0	1/1	0/0	0/0	0/0	0.008/0.040	0.028/n	0.742/0.696	0.230/n	0.177/0.264	0.060/0.231	0/0.169	0/0.044
0.1	0.1	0.315	0	1/1	0/0	0/0	0.001/0.060	0.024/0.076	0.078/n	0.712/0.688	0.210/n	0.167/0.235	0.062/0.217	0.000/0.162	0/0.039
0.1	1.0	0.315	0	1/1	0/0	0/0.096	0.026/0.137	0.108/0.144	0.139/n	0.697/0.686	0.164/n	0.139/0.170	0.061/0.162	0.000/0.130	0/0.048
0.1	2.0	0.310	0	1/1	0/0.046	0/0.125	0.066/0.156	0.134/0.162	0.158/n	0.699/0.691	0.143/n	0.121/0.147	0.052/0.141	0/0.111	0/0.037
0.5	0	0.336	0	1/1	0/0	0/0	0.011/0	0.035/0	0.052/0	0.744/0.695	0.204/n	0.160/0.305	0.058/0.240	0/0.181	0/0.058
0.5	0.01	0.344	0	1/1	0/0	0/0	0.015/0	0.038/0.042	0.065/n	0.720/0.669	0.214/n	0.162/0.289	0.058/0.252	0/0.186	0/0.056
0.5	0.1	0.343	0	1/1	0/0	0/0	0.014/0.066	0.050/0.088	0.101/n	0.692/0.661	0.207/n	0.160/0.251	0.061/0.233	0/0.173	0/0.055
0.5	1.0	0.340	0	1/1	0/0	0/0.099	0.032/0.138	0.111/0.145	0.151/n	0.669/0.660	0.180/n	0.145/0.195	0.068/0.189	0/0.145	0/0.059
0.5	2.0	0.337	0	1/1	0/0.048	0/0.135	0.065/0.171	0.149/0.175	0.181/n	0.671/0.664	0.148/n	0.123/0.161	0.059/0.156	0.000/0.123	0/0.050
0.5	5.0	0.328	0	1/1	0/0.109	0.001/0.169	0.121/0.198	0.177/0.202	0.199/n	0.680/0.673	0.121/n	0.099/0.124	0.041/0.120	0/0.095	0/0.034
0.5	10.0	0.315	0	1/1	0/0.118	0.006/0.175	0.131/0.200	0.180/0.205	0.201/n	0.694/0.686	0.105/n	0.087/0.109	0.042/0.103	0/0.085	0/0.032
0.9	0	0.409	0	1/1	0/0	0/0	0.036/0	0.093/0	0.138/0	0.655/0.617	0.208/n	0.160/0.383	0.072/0.293	0/0.214	0/0.089
0.9	0.01	0.399	0	1/1	0/0	0/0	0.038/0	0.095/0.055	0.150/n	0.654/0.612	0.196/n	0.145/0.332	0.061/0.286	0/0.206	0/0.088
0.9	0.1	0.397	0	1/1	0/0	0.000/0	0.039/0.080	0.099/0.098	0.169/n	0.625/0.609	0.205/n	0.144/0.292	0.062/0.277	0/0.203	0/0.085
0.9	1.0	0.392	0	1/1	0/0	0.001/0.111	0.044/0.158	0.128/0.165	0.188/n	0.617/0.610	0.195/n	0.150/0.225	0.071/0.221	0/0.173	0/0.087
0.9	2.0	0.384	0	1/1	0/0.051	0.001/0.131	0.066/0.172	0.145/0.177	0.187/n	0.627/0.616	0.187/n	0.152/0.206	0.069/0.202	0/0.163	0/0.081
0.9	5.0	0.368	0	1/1	0/0.110	0.002/0.180	0.117/0.207	0.187/0.213	0.215/n	0.643/0.632	0.142/n	0.119/0.154	0.055/0.149	0.000/0.125	0/0.063
0.9	10.0	0.340	0	1/1	0/0.148	0.015/0.196	0.153/0.216	0.204/0.221	0.227/n	0.670/0.661	0.103/n	0.081/0.118	0.036/0.113	0/0.088	0/0.039
0.999	0	[a]0.658	0.316	1/1	0/0	0/0	0/0	0.001/0	0.055/0	0.498/0.514	0.448/n	0.122/0.486	0.028/0.324	0/0.186	0/0.082
1.000	0.1	[a]0.658	0.315	1/1	0/0	0/0	0.151/0.003	0.220/0.080	n/0.482	0.362/0.438	n/0.138	0.418/0.034	0.352/0	0.211/0	0.095
1.009	1.0	[a]0.658	0.515	1/1	0/0	0/0.120	0/0.266	0.034/0.292	0.178/n	0.493/0.350	0.329/n	0.128/0.357	0.040/0.327	0/0.209	0/0.086
1.019	2.0	[a]0.658	0.608	1/1	0/0.016	0/0.140	0/0.287	0.044/0.322	0.210/n	0.531/0.351	0.259/n	0.101/0.327	0.038/0.290	0/0.169	0/0.081
1.049	5.0	[a]0.658	0.650	1/1	0/0.010	0/0.057	0.002/0.257	0.015/0.340	0.145/n	0.676/0.368	0.178/n	0.038/0.292	0.024/0.212	0/0.063	0/0.032
1.099	10.0	[a]0.658	0.633	1/1	0/0.034	0/0.133	0.020/0.289	0.060/0.331	0.246/n	0.512/0.356	0.242/n	0.075/0.313	0.041/0.277	0.001/0.153	0/0.053

[a]Trajectories determined by fixed step size.

TABLE IV. - PROBABILITY DISTRIBUTIONS FOR ΔH_{BC} AND $\Delta|\bar{M}_{BC}|^2$ PER COLLISION THROUGH A RANGE OF HEAT BATH TEMPERATURES

[Entry n means given interval is within noise level; all entries except $H_{BC}^{(i)} = 0.5\ D_e$, $|\bar{M}_{BC}|^{2(i)} = 0$, $T(A_r) = 1800$ K are based on 1000 RCOL; an estimate of reliability for fractional populations is ±0.01.]

$\frac{H_{BC}^{(i)}}{D_e}$	$\lvert\bar{M}_{BC}\rvert^{2(i)}$	$\frac{\sum(\text{RCOL})}{\sum(\text{RCOL}+\text{NCOL})}$	Temperature, K	$w_1 = \int_x^y f(\Delta H_{BC})d(\Delta H_{BC})$	$w_2 = \int_x^y f\left(\Delta\lvert\bar{M}_{BC}\rvert^2\right)d\left(\Delta\lvert\bar{M}_{BC}\rvert^2\right)$

w_1/w_2

				Integral lower limit, y											
				$-\infty$	$-\infty$	$-\infty$	$-\infty$	$-\infty$	-n	0.0001	0.001	0.01	0.1	1.0	10.0
				Integral upper limit, y											
				-1.0	-0.1	-0.01	-0.001	-0.0001	n	∞	∞	∞	∞	∞	∞
0	0	[a]0.309	300	0/0	0/0	0/0	0/0	0/0	0.719/0.697	0.281/n	0.178/0.303	0.007/0.272	0/0.140	0/0.001	0/0
0	0	[a]0.309	1000	0/0	0/0	0/0	0/0	0/0	0.744/0.709	0.256/n	0.193/0.291	0.042/0.249	0/0.173	0/0.019	0/0
0	0	[a]0.308	1800	0/0	0/0	0/0	0/0	0/0	0.760/0.721	0.240/n	0.189/0.279	0.062/0.233	0/0.173	0/0 042	0/0
0	0	[a]0.309	3000	0/0	0/0	0/0	0/0	0/0	0.770/0.732	0.230/n	0.186/0.268	0.083/0.223	0.002/0.172	0/0.058	0/0
0	0	[a]0.309	5000	0/0	0/0	0/0	0/0	0/0	0.779/0.747	0.221/n	0.184/0.253	0.099/0.215	0.006/0.172	0/0.076	0/0.001
0	0	[a]0.309	10000	0/0	0/0	0/0	0/0	0/0	0.787/0.762	0.213/n	0.179/0.238	0.117/0.205	0.024/0.168	0/0.097	0/0.008
0.5	0	0.340	300	0/0	0/0	0/0	0.018/0	0.044/0	0.697/0.668	0.258/n	0.162/0.332	0.007/0.296	0/0.171	0/0.006	0/0
0.5	0	0.347	1000	0/0	0/0	0.004/0	0.028/0	0.047/0	0.716/0.671	0.236/n	0.177/0.329	0.040/0.272	0/0.190	0/0.035	0/0
0.5	0	0.336	1800	0/0	0/0	0.011/0	0.035/0	0.052/0	0.744/0.695	0.204/n	0.160/0.305	0.058/0.240	0/0.181	0/0.058	0/0
0.5	0	0.349	3000	0/0	0/0	0.018/0	0.048/0	0.072/0	0.737/0.695	0.191/n	0.156/0.305	0.075/0.237	0.003/0.186	0/0.077	0/0.001
0.5	0	0.349	10000	0/0	0.000/0	0.026/0	0.056/0	0.102/0	0.721/0.735	0.177/n	0.152/0.265	0.108/0.217	0.023/0.179	0/0.107	0/0.014
0.5	1.0	0.345	300	0/0	0/0.188	0.044/0.213	0.198/0.216	0.219/n	0.660/0.656	0.121/n	0.093/0.128	0.004/0.123	0/0.092	0/0.005	0/0
0.5	1.0	0.344	1000	0/0	0/0.131	0.037/0.170	0.141/0.174	0.174/n	0.664/0.657	0.163/n	0.124/0.170	0.044/0.165	0/0.129	0/0.038	0/0
0.5	1.0	0.340	1800	0/0	0/0.099	0.032/0.138	0.111/0.145	0.151/n	0.669/0.660	0.180/n	0.145/0.195	0.068/0.189	0/0.145	0/0.059	0/0
0.5	1.0	0.346	3000	0/0	0/0.089	0.032/0.143	0.103/0.151	0.149/n	0.671/0.657	0.180/n	0.147/0.192	0.079/0.187	0.004/0.147	0/0.076	0/0.001
0.5	1.0	0.346	10000	0/0	0.002/0.056	0.032/0.105	0.074/0.121	0.129/n	0.679/0.658	0.192/n	0.155/0.221	0.111/0.206	0.026/0.155	0/0.103	0/0.018
0.5	5.0	0.328	1800	0/0.109	0.001/0.169	0.121/0.198	0.177/0.202	0.199/n	0.680/0.673	0.121/n	0.099/0.124	0.041/0.120	0/0.095	0/0.034	0/0
0.5	5.0	0.328	10000	0/0.060	0.003/0.102	0.063/0.142	0.104/0.149	0.139/n	0.685/0.673	0.176/n	0.142/0.178	0.101/0.171	0.028/0.133	0/0.089	0/0.019
0.5	10.0	0.315	1800	0/0.118	0.006/0.175	0.131/0.200	0.180/0.205	0.201/n	0.694/0.686	0.105/n	0.087/0.109	0.042/0.103	0/0.085	0/0.032	0/0
0.5	10.0	0.314	10000	0/0.086	0.009/0.123	0.091/0.157	0.125/0.163	0.154/n	0.695/0.686	0.151/n	0.125/0.151	0.092/0.145	0.024/0.115	0/0.079	0/0.013
0.5	0.25	0.343	300	0/0	0/0.078	0.001/0.139	0.109/0.146	0.156/n	0.668/0.658	0.176/n	0.128/0.196	0.007/0.188	0/0.133	0/0.004	0/0
0.5	0.82	0.343	1000	0/0	0/0.115	0.029/0.152	0.135/0.158	0.166/n	0.669/0.659	0.165/n	0.132/0.183	0.042/0.175	0/0.135	0/0.037	0/0
0.5	1.48	0.341	1800	0/0.031	0/0.123	0.049/0.159	0.134/0.165	0.166/n	0.669/0.660	0.165/n	0.134/0.175	0.063/0.169	0.000/0.133	0/0.057	0/0
0.5	8.24	0.321	10000	0/0.082	0.007/0.119	0.082/0.152	0.121/0.161	0.151/n	0.690/0.680	0.159/n	0.131/0.159	0.092/0.152	0.025/0.120	0/0.082	0/0.015

[a]Trajectories determined by fixed step size.

TABLE V. - CORRESPONDENCE (FRACTION OF RCOL) BETWEEN GAINS AND LOSSES IN H_{BC} AND $|\vec{M}_{BC}|^2$ FOR T = 1800 K

$\Delta|\vec{M}_{BC}|^2$

ΔH_{BC}	Gains	Losses
Gains	(g, g)	(g, ℓ)
Losses	(ℓ, g)	(ℓ, ℓ)

g = Gains
ℓ = Losses

$\left(H_{BC(i)}, |\vec{M}_{BC}|^{2(i)}\right)$

1.000	0			
0	0			
(0, 0)				
0.849	0	0.782	0.011	0.700	0.011	0.528	0.017	0.470	0.004
0.151	0	0.075	0.132	0.051	0.238	0.015	0.440	0.007	0.519
(0.1 D_e, 0)		(0.1 D_e, 0.01)		(0.1 D_e, 0.1)		(0.1 D_e, 1.0)		(0.1 D_e, 2.0)	
0.762	0	0.685	0.023	0.612	0.039	0.507	0.036	0.420	0.035
0.238	0	0.172	0.120	0.125	0.224	0.068	0.389	0.059	0.486
(0.5 D_e, 0)		(0.5 D_e, 0.01)		(0.5 D_e, 0.1)		(0.5 D_e, 1.0)		(0.5 D_e, 2.0)	
0.353	0.030	0.320	0.022	0.593	0	0.504	0.045	0.485	0.055
0.029	0.588	0.027	0.631	0.407	0	0.344	0.107	0.262	0.198
(0.5 D_e, 5.0)		(0.5 D_e, 10.0)		(0.9 D_e, 0)		(0.9 D_e, 0.01)		(0.9 D_e, 0.1)	
0.433	0.075	0.412	0.088	0.306	0.094	0.261	0.054	0.790	0
0.144	0.348	0.126	0.374	0.114	0.486	0.087	0.598	0.210	0
(0.9 D_e, 1.0)		(0.9 D_e, 2.0)		(0.9 D_e, 5.0)		(0.9 D_e, 10.0)		(0.999 D_e, 0)	
0.548	0.190	0.473	0.121	0.419	0.080	0.338	0.093	0.428	0.037
0.104	0.158	0.078	0.328	0.089	0.412	0.130	0.439	0.056	0.479
(1.000 D_e, 0.1)		(1.009 D_e, 1.0)		(1.019 D_e, 2.0)		(1.049 D_e 5.0)		(1.099 D_e, 10.0)	

TABLE VI. - CORRESPONDENCE (FRACTION OF RCOL) BETWEEN LARGE AND SMALL GAINS AND LOSSES IN H_{BC} AND $|\vec{M}_{BC}|^2$ FOR T = 1800 K

Sub-division	$\lvert\Delta H_{BC}\rvert$	$\Delta\lvert\vec{M}_{BC}\rvert^2$
1	<0.01	<0.1
2	<.01	≥.1
3	≥.01	<.1
4	≥.01	≥.1

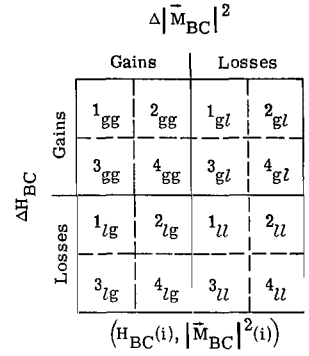

0.437	0.361	0	0
0	0.202	0	0
0	0	0	0
0	0	0	0

(0, 0)

0.326	0.328	0	0
0	0.195	0	0
0.136	0.014	0	0
0.001	0	0	0

(0.1 D_e, 0)

0.258	0.334	0.011	0
0	0.190	0	0
0.062	0.013	0.132	0
0	0	0	0

(0.1 D_e, 0.01)

0.203	0.300	0.010	0
0	0.197	0.001	0
0.034	0.015	0.238	0
0.001	0.001	0	0

(0.1 D_e, 0.1)

0.117	0.216	0.014	0.003
0.001	0.194	0	0
0.011	0.004	0.140	0.219
0	0	0	0.081

(0.1 D_e, 1.0)

0.111	0.191	0.001	0.003
0	0.168	0	0
0.007	0	0.118	0.188
0	0	0	0.213

(0.1 D_e, 2.0)

0.314	0.277	0	0
0.003	0.168	0	0
0.141	0.063	0	0
0.004	0.030	0	0

(0.5 D_e, 0)

0.232	0.285	0.023	0
0.003	0.165	0	0
0.078	0.051	0.120	0
0.004	0.039	0	0

(0.5 D_e, 0.01)

0.181	0.253	0.038	0
0.003	0.175	0.001	0
0.043	0.045	0.219	0
0.006	0.031	0.005	0

(0.5 D_e, 0.1)

0.118	0.195	0.012	0.017
0.005	0.189	0.002	0.005
0.023	0.029	0.118	0.193
0.004	0.012	0.002	0.076

(0.5 D_e, 1.0)

0.096	0.159	0.009	0.016
0.001	0.164	0.002	0.008
0.015	0.028	0.108	0.202
0.003	0.013	0.002	0.174

(0.5 D_e, 2.0)

0.085	0.150	0.014	0.010
0	0.118	0.001	0.005
0.006	0.014	0.086	0.141
0.001	0.008	0.002	0.359

$(0.5\ D_e,\ 5.0)$

0.063	0.128	0.010	0.009
0.001	0.128	0.001	0.002
0.014	0.013	0.086	0.130
0	0	0	0.415

$(0.5\ D_e, 10.0)$

0.238	0.179	0	0
0.007	0.169	0	0
0.220	0.098	0	0
0.011	0.078	0	0

$(0.9\ D_e, 0)$

0.173	0.179	0.043	0
0.005	0.147	0.002	0
0.142	0.108	0.105	0
0.011	0.083	0.002	0

$(0.9\ D_e, 0.01)$

0.143	0.190	0.050	0
0.005	0.147	0.005	0
0.080	0.092	0.191	0
0.008	0.082	0.007	0

$(0.9\ D_e, 0.1)$

0.081	0.186	0.021	0.040
0.007	0.159	0.003	0.011
0.041	0.051	0.112	0.176
0.007	0.045	0.004	0.056

$(0.9\ D_e, 1.0)$

0.070	0.182	0.022	0.047
0.002	0.158	0.004	0.015
0.038	0.045	0.092	0.153
0.005	0.038	0.004	0.125

$(0.9\ D_e, 2.0)$

0.049	0.128	0.026	0.047
0	0.129	0.001	0.020
0.026	0.050	0.060	0.146
0.004	0.034	0.004	0.276

$(0.9\ D_e, 5.0)$

0.064	0.103	0.015	0.028
0.002	0.092	0.001	0.010
0.021	0.047	0.058	0.109
0.001	0.018	0.001	0.430

$(0.9\ D_e, 10.0)$

0.515	0.232	0	0
0	0.043	0	0
0.202	0.008	0	0
0	0	0	0

$(0.999\ D_e, 0)$

0.240	0.257	0.190	0
0	0.051	0	0
0.092	0.012	0.158	0
0	0	0	0

$(1.000\ D_e, 0.1)$

0.165	0.247	0.107	0.014
0	0.061	0	0
0.069	0.009	0.160	0.168
0	0	0	0

$(1.009\ D_e, 1.0)$

0.169	0.192	0.063	0.017
0	0.058	0	0
0.083	0.006	0.216	0.196
0	0	0	0

$(1.019\ D_e, 2.0)$

0.247	0.054	0.088	0.005
0	0.037	0	0
0.126	0.004	0.357	0.079
0	0	0	0.003

$(1.049\ D_e, 5.0)$

0.196	0.169	0.035	0.002
0	0.063	0	0
0.055	0.001	0.279	0.170
0	0	0	0.030

$(1.099\ D_e, 10.0)$

TABLE VII. - CORRESPONDENCE (FRACTION OF RCOL) BETWEEN LARGE AND SMALL GAINS AND LOSSES IN H_{BC} AND $|\vec{M}_{BC}|^2$ THROUGH A RANGE OF HEAT BATH TEMPERATURE

Sub-division	$\lvert\Delta H_{BC}\rvert$	$\lvert\Delta\lvert\vec{M}_{BC}\rvert^2\rvert$
1	<0.01	<0.1
2	<.01	≥.1
3	≥.01	<.1
4	≥.01	≥.1

$\Delta|\vec{M}_{BC}|^2$

ΔH_{BC}		Gains		Losses	
Gains		$^1_{gg}$	$^2_{gg}$	$^1_{gl}$	$^2_{gl}$
		$^3_{gg}$	$^4_{gg}$	$^3_{gl}$	$^4_{gl}$
Losses		$^1_{lg}$	$^2_{lg}$	$^1_{ll}$	$^2_{ll}$
		$^3_{lg}$	$^4_{lg}$	$^3_{ll}$	$^4_{ll}$

$(H_{BC}(i), |\vec{M}_{BC}|^2(i), T)$

0.546	0.432	0	0
0	0.022	0	0
0	0	0	0
0	0	0	0

(0, 0, 300)

0.441	0.423	0	0
0	0.136	0	0
0	0	0	0
0	0	0	0

(0, 0, 1000)

0.437	0.361	0	0
0	0.202	0	0
0	0	0	0
0	0	0	0

(0, 0, 1800)

0.443	0.288	0	0
0	0.269	0	0
0	0	0	0
0	0	0	0

(0, 0, 3000)

0.443	0.235	0	0
0	0.322	0	0
0	0	0	0
0	0	0	0

(0, 0, 5000)

0.454	0.166	0	0
0.003	0.377	0	0
0	0	0	0
0	0	0	0

(0, 0, 10 000)

0.342	0.449	0	0
0	0.022	0	0
0.155	0.032	0	0
0	0	0	0

(0.5 D_e, 0, 300)

0.323	0.366	0	0
0.001	0.115	0	0
0.126	0.058	0	0
0.003	0.008	0	0

(0.5 D_e, 0, 1000)

0.314	0.277	0	0
0.003	0.168	0	0
0.141	0.063	0	0
0.004	0.030	0	0

(0.5 D_e, 0, 1800)

0.246	0.201	0	0
0.003	0.211	0	0
0.213	0.074	0	0
0.005	0.047	0	0

(0.5 D_e, 0, 3000)

0.165	0.097	0	0
0.008	0.302	0	0
0.302	0.052	0	0
0.013	0.061	0	0

$(0.5\ D_e, 0, 10\ 000)$

0.075	0.241	0.019	0.010
0	0.013	0	0
0.029	0.013	0.064	0.407
0	0.001	0	0.128

$(0.5\ D_e, 1.0, 300)$

0.107	0.214	0.015	0.022
0	0.126	0	0.001
0.011	0.026	0.109	0.261
0.001	0.008	0.003	0.096

$(0.5\ D_e, 1.0, 1000)$

0.118	0.195	0.012	0.017
0.005	0.189	0.002	0.005
0.023	0.029	0.118	0.193
0.004	0.012	0.002	0.076

$(0.5\ D_e, 1.0, 1800)$

0.112	0.158	0.023	0.024
0.001	0.218	0.004	0.006
0.019	0.030	0.154	0.158
0.002	0.019	0.003	0.069

$(0.5\ D_e, 1.0, 3000)$

0.135	0.091	0.023	0.023
0.005	0.293	0.003	0.019
0.049	0.025	0.162	0.078
0.006	0.039	0.008	0.041

$(0.5\ D_e, 1.0, 10\ 000)$

0.085	0.150	0.014	0.010
0	0.118	0.001	0.005
0.006	0.014	0.086	0.141
0.001	0.008	0.002	0.359

$(0.5\ D_e, 5.0, 1800)$

0.107	0.092	0.020	0.027
0.003	0.284	0.003	0.017
0.029	0.015	0.118	0.094
0.001	0.014	0.003	0.173

$(0.5\ D_e, 5.0, 10\ 000)$

0.063	0.128	0.010	0.009
0.001	0.128	0.001	0.002
0.014	0.013	0.086	0.130
0	0	0	0.415

$(0.5\ D_e, 10.0, 1800)$

0.102	0.079	0.016	0.008
0	0.278	0	0.013
0.011	0.007	0.114	0.084
0.001	0.001	0	0.286

$(0.5\ D_e, 10.0, 10\ 000)$

0.137	0.338	0.030	0.004
0	0.021	0	0
0.049	0.029	0.168	0.222
0	0	0	0.002

$(0.5\ D_e, 0.25, 300)$

0.107	0.234	0.010	0.022
0.001	0.119	0.001	0.003
0.032	0.032	0.116	0.237
0.002	0.008	0.003	0.073

$(0.5\ D_e, 0.82, 1000)$

0.096	0.174	0.014	0.030
0	0.176	0.001	0.006
0.026	0.023	0.107	0.203
0.003	0.017	0.002	0.122

$(0.5\ D_e, 1.48, 1800)$

0.108	0.091	0.014	0.017
0.001	0.267	0.003	0.014
0.015	0.009	0.110	0.096
0.001	0.006	0.004	0.244

$(0.5\ D_e, 8.24, 10\ 000)$

TABLE VIII. - VALUES OF $|\vec{M}_{BC}|^2(i)$ REQUIRED FOR ΔH_{BC} AND $\Delta|\vec{M}_{BC}|^2$ GAIN-LOSS BALANCES AND COMPARISON WITH $\langle|\vec{M}_{BC}|^2\rangle$ FOR EQUILIBRIUM RIGID ROTATORS

$H_{BC}(i)$	Temperature, T, K	$\|\vec{M}_{BC}\|^2(i)$ for vibrating rotator		$\langle\|\vec{M}_{BC}\|^2\rangle$ for rigid rotators with $\|\vec{R}_{BC}\|^2$ =					Rotational temperature, K
		Balance for, ΔH_{BC}	Balance for, $\Delta\|\vec{M}_{BC}\|^2$	$\|\vec{R}_{BC}(e)\|^2$	[a]5.27(1)	[a]5.62(5)	[a]8.9(7)	$\langle\|\vec{R}_{BC}\|^2\rangle_{min}$	
0.1 D_e	1 800	1.53±0.06	1.50±0.06	0.286	0.290	0.309	0.493	0.238	300
.5 D_e	300	.30±0.03	.36±0.06	.477	.483	.515	.821	.397	500
.5 D_e	1 000	.79±0.02	.98±0.02	.954	.966	1.03	1.64	.794	1 000
.5 D_e	1 800	1.45±0.02	1.73±0.02	1.72	1.74	1.86	2.96	1.43	1 800
.5 D_e	10 000	9.46±0.03	7.90±0.03	4.77	4.83	5.15	8.21	3.97	5 000
.9 D_e	1 800	2.00±0.00	2.30±0.11	9.54	9.66	10.3	16.4	7.94	10 000

[a]For the vibrating-rotator $\langle|\vec{R}_{BC}|^2\rangle$ = 5.27(1) Å^2 at 0.1 D_e, 5.62(5) Å^2 at 0.5 D_e, 8.9(7)Å^2 at 0.9 D_e (see discussion accompanying eq. (9)). $\langle|\vec{R}_{BC}|^2\rangle_{min} \approx 4.33$ Å^2 calculated from average of $|\vec{R}_{BC}|_{min}$ at $V_1 = 0.1\ D_e$ and 0.5 D_e. Because of vibration-rotation coupling, $|\vec{R}_{BC}|_{min}$ at $H_{BC} = 0.5\ D_e$ is not equal to $|\vec{R}_{BC}|_{min}$ at $V_1 = 0.5\ D_e$, except for $|\vec{M}_{BC}|^2 = 0$.

TABLE IX. - PROBABILITY DISTRIBUTIONS AND MATRIX TABULATIONS OF ΔH_{BC} AND $\Delta|\bar{M}_{BC}|^2$ FOR TRAJECTORIES CALCULATED WITH ATTRACTIVE PART OF V_2 REMOVED

$\frac{H_{BC}^{(i)}}{D_e}$	$\lvert\bar{M}_{BC}\rvert^{2(i)}$	$\frac{\sum(\text{RCOL})}{\sum(\text{RCOL}+\text{NCOL})}$	Temperature, T, K	$w_1 = \int_x^y f(\Delta H_{BC})d(\Delta H_{BC})$	$w_2 = \int_x^y f\left(\Delta\lvert\bar{M}_{BC}\rvert^2\right)d\left(\Delta\lvert\bar{M}_{BC}\rvert^2\right)$

w_1/w_2

				Integral lower limit, x											
				$-\infty$	$-\infty$	$-\infty$	$-\infty$	$-\infty$	-n	0.0001	0.001	0.01	0.1	1.0	10.0
				Integral upper limit, y											
				-1.0	-0.1	-0.01	-0.001	-0.0001	n	∞	∞	∞	∞	∞	∞
0.5	0.25	0.348	300	0/0	0 / 0.062	0 / 0.150	0.075 / 0.170	0.171 / n	0.690 / 0.659	0.139 / n	0.076 / 0.171	0.002 / 0.152	0 / 0.070	0 / 0.001	0/0
0.5	1.48	0.342	1800	0/0.021	0 / 0.120	0.034 / 0.166	0.132 / 0.174	0.171 / n	0.675 / 0.660	0.154 / n	0.120 / 0.166	0.047 / 0.155	0.000 / 0.116	0 / 0.040	0/0
0.5	8.24	0.319	10000	0/0.075	0.006 / 0.129	0.079 / 0.154	0.130 / 0.158	0.151 / n	0.690 / 0.682	0.159 / n	0.141 / 0.159	0.089 / 0.154	0.021 / 0.131	0 / 0.080	0 / 0.012

0.251	0.195	0	0
0	0.007	0	0
0.051	0	0.318	0.718
0	0	0	0

($0.5\ D_e$, 0.25, 300)

0.132	0.188	0.009	0.011
0	0.137	0	0.001
0.017	0.010	0.150	0.247
0.001	0.004	0	0.093

($0.5\ D_e$, 1.48, 1800)

0.080	0.129	0.013	0.014
0.003	0.266	0	0.010
0.008	0.010	0.081	0.139
0	0.004	0.001	0.242

($0.5\ D_e$, 8.24, 10 000)

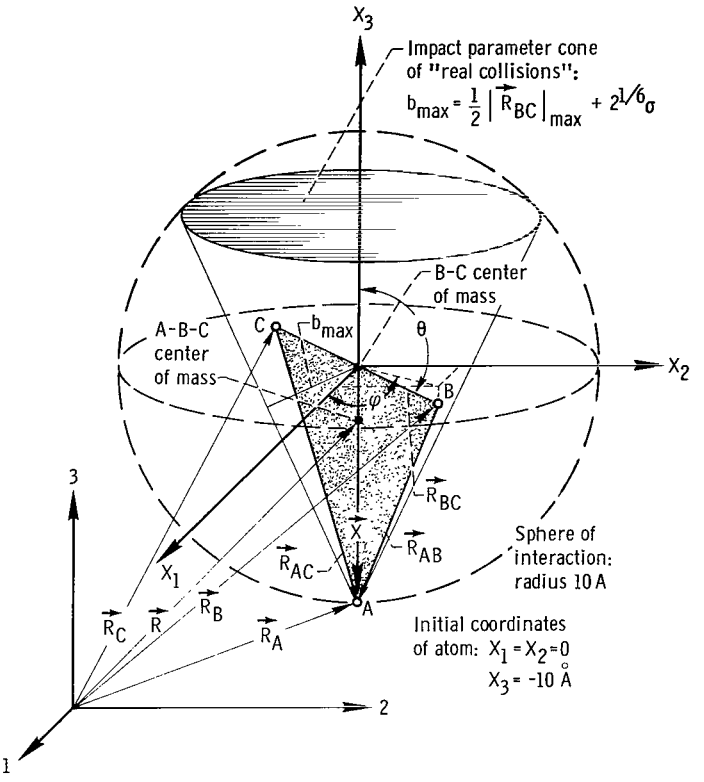

Figure 1. - Coordinate system for 3-body problem.

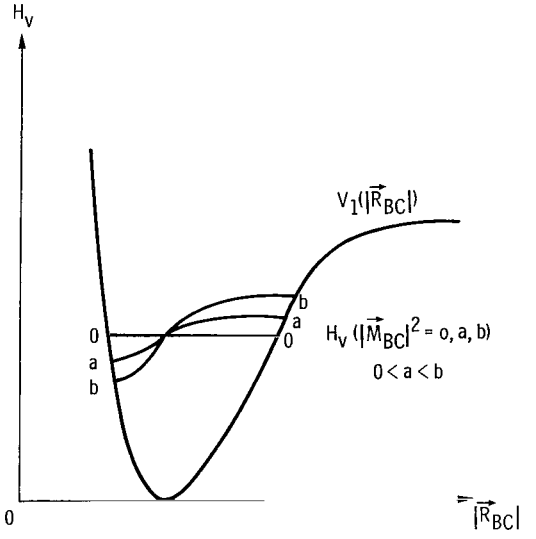

Figure 2. - Classical visualization of effect of rotation on vibrational energy, drawn for a fixed value of H_v at $|\vec{R}_{BC}^{(e)}|$.

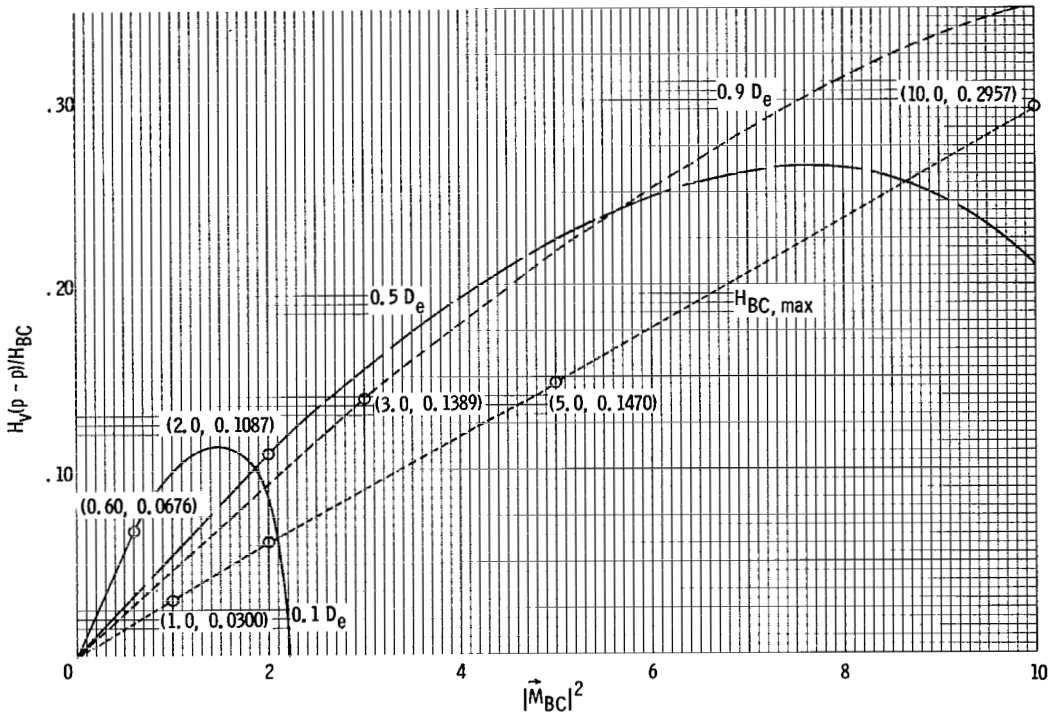

Figure 3. - Vibration rotation coupling amplitude in free Br_2 as function of angular momentum.

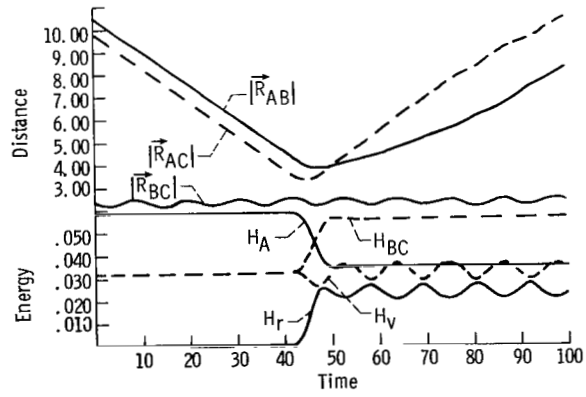

Figure 4. - Atom-molecule trajectory.

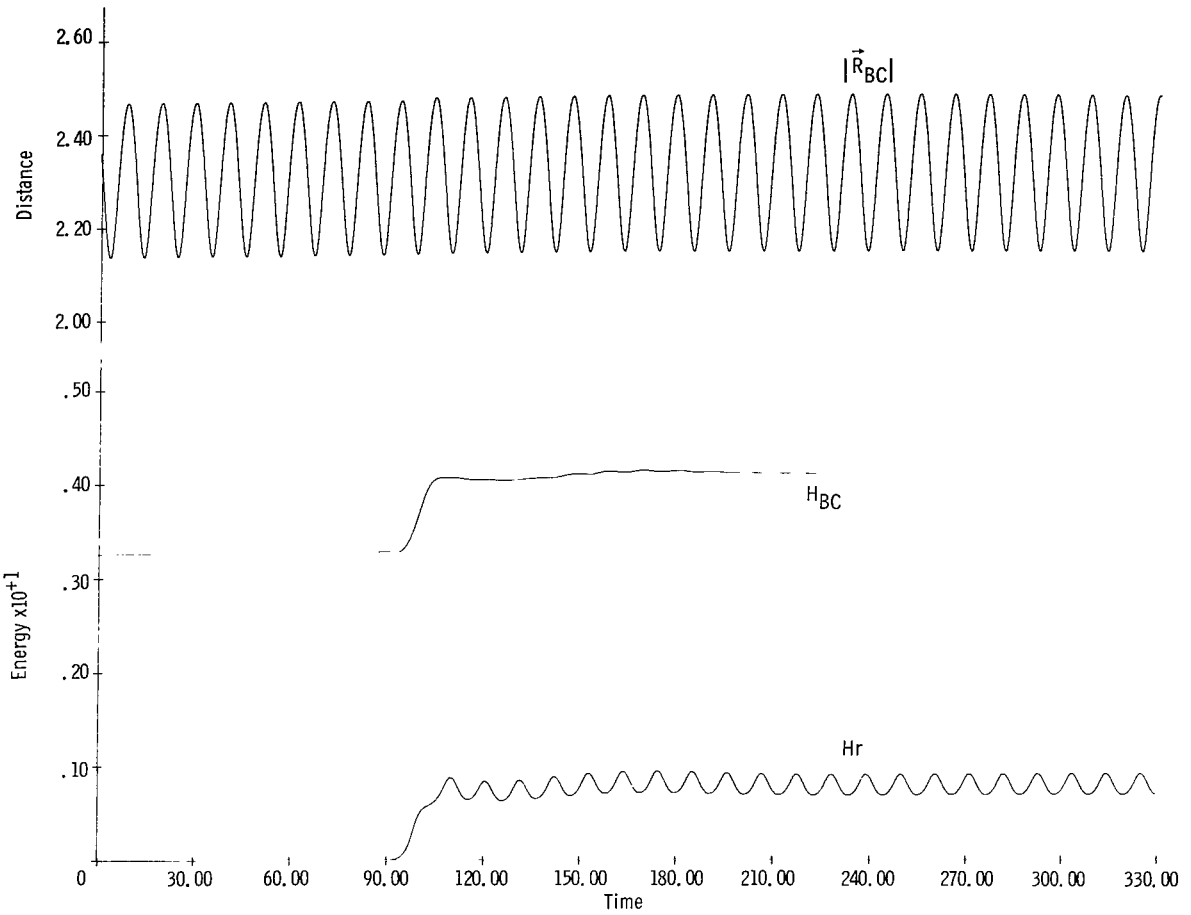

(a) Trajectory with initial atom velocity scaled to 300 K.

Figure 5. - Trajectories with various initial atom velocities.

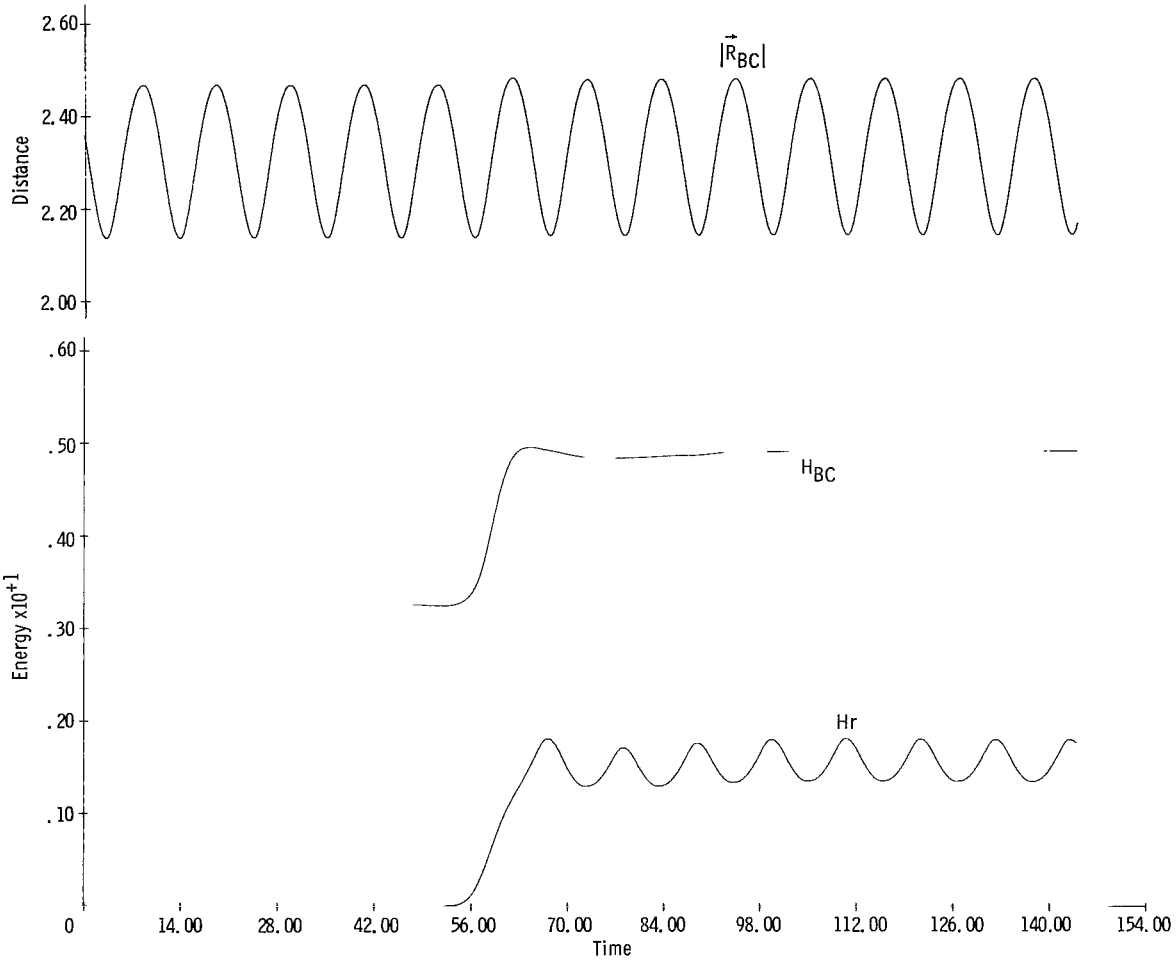

(b) Trajectory with initial atom velocity scaled to 1000 K.

Figure 5. - Continued.

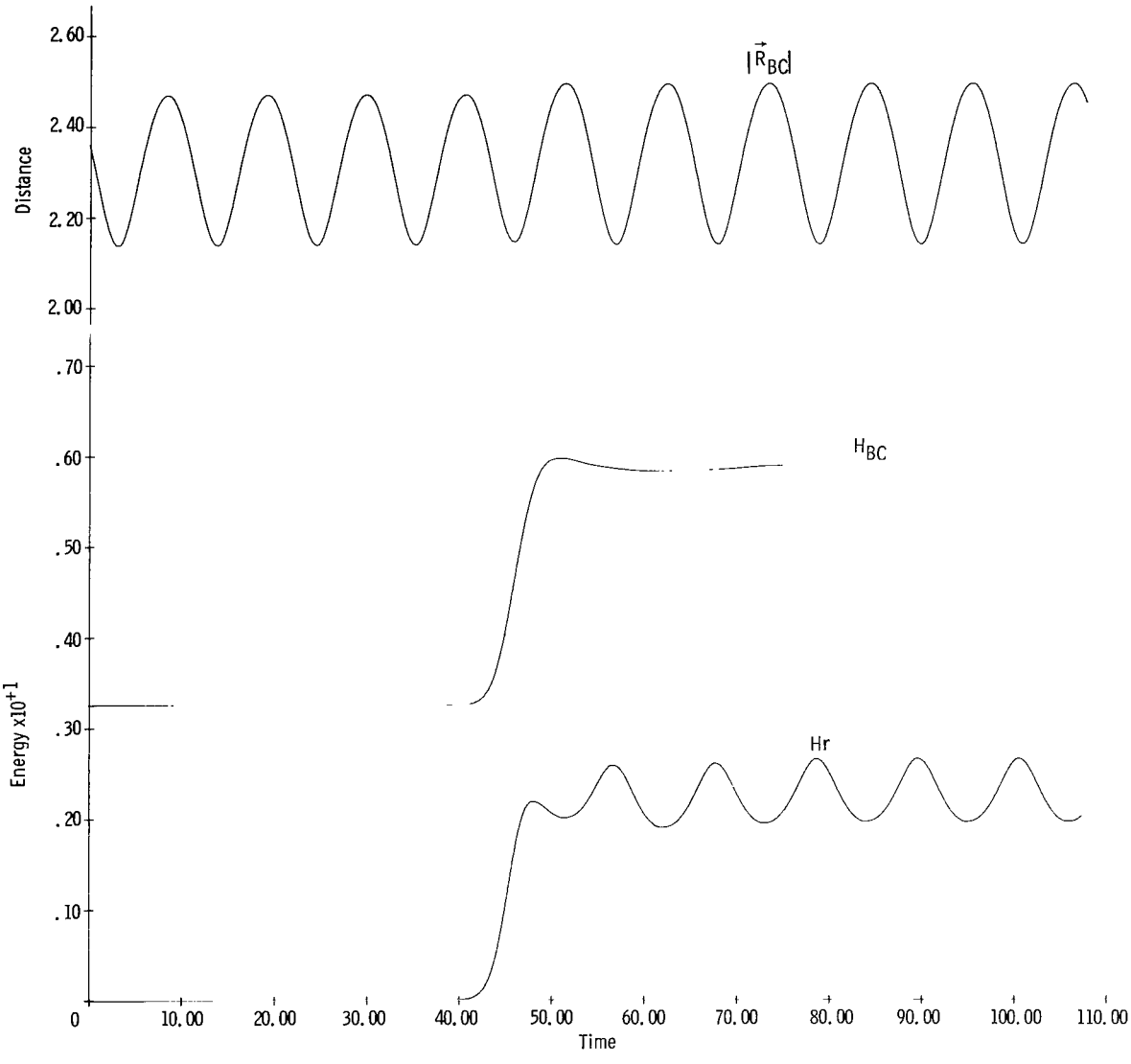

(c) Trajectory with initial atom velocity scaled to 1800 K.

Figure 5. - Continued.

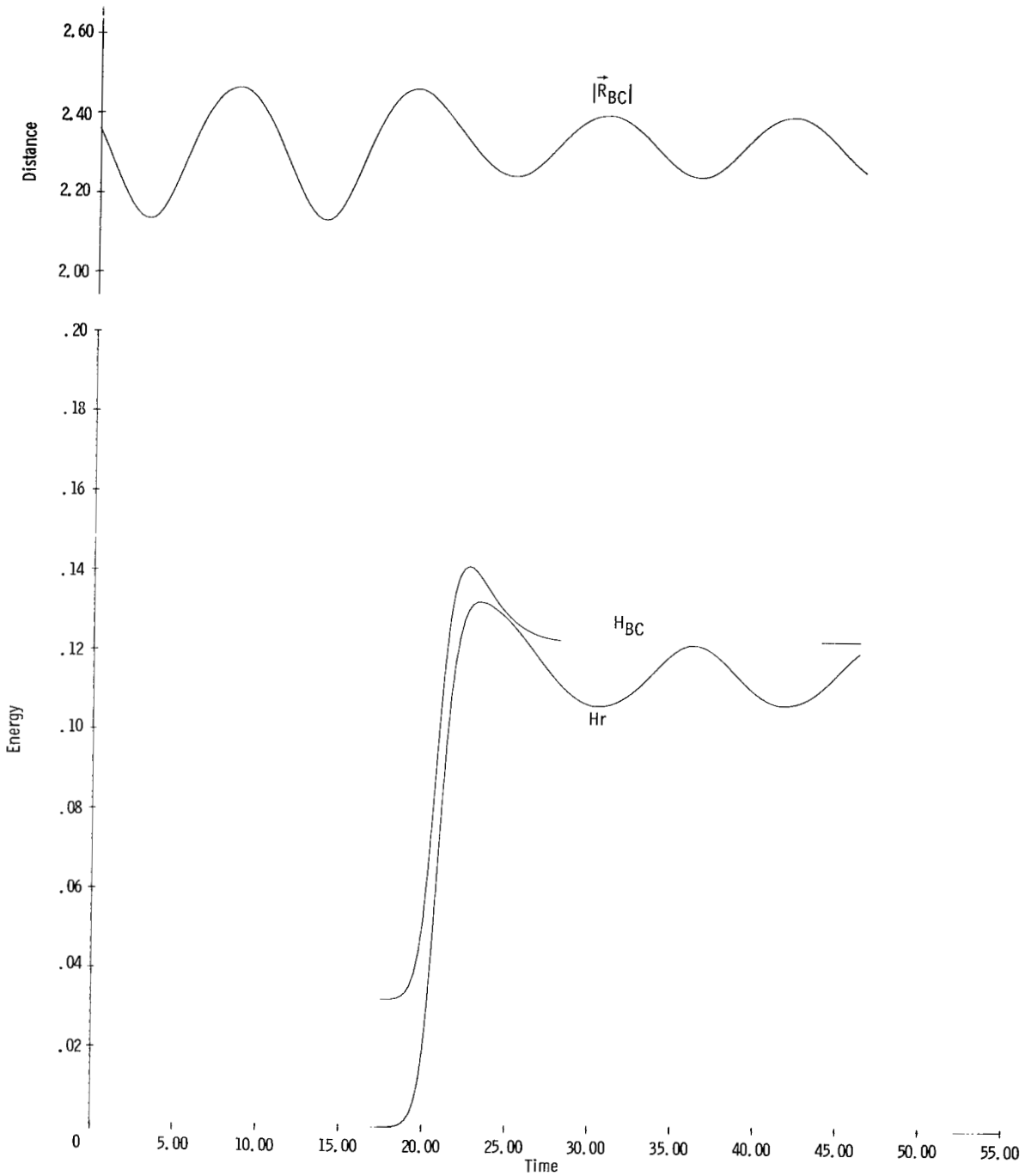

(d) Trajectory with initial atom velocity scaled to 10 000 K.

Figure 5. - Concluded.

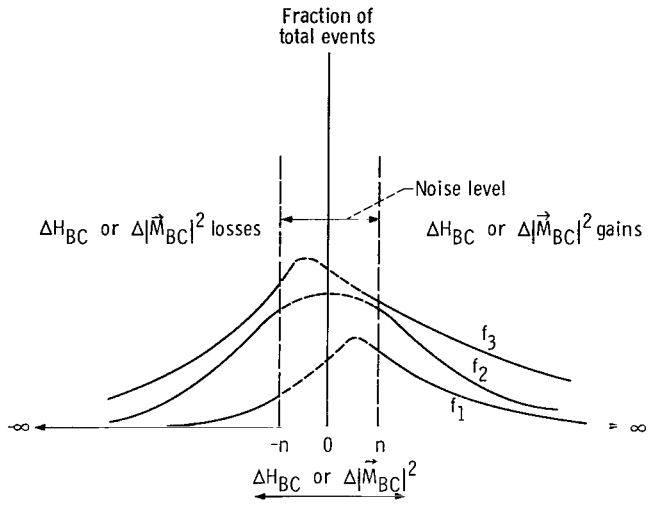

Figure 6. - Schematic drawing of a family of probability distributions for internal energy changes, ΔH_{BC}, or angular momentum changes, $\Delta|\vec{M}_{BC}|^2$, per collision.

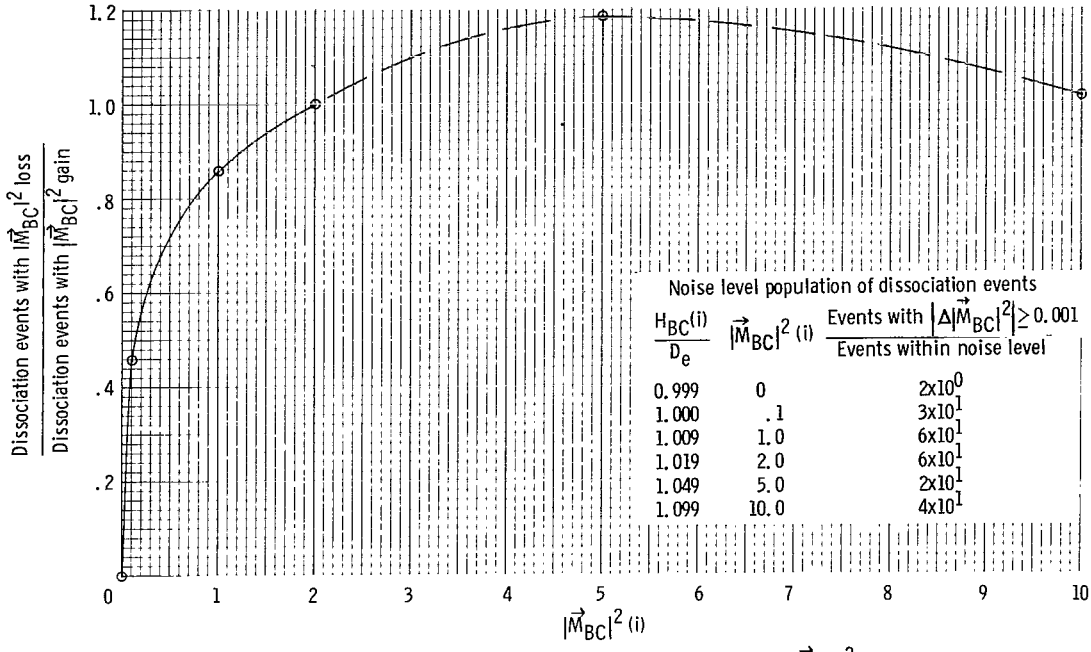

Figure 7. - Comparison of dissociation events with gain or loss in $|\vec{M}_{BC}|^2$ (T = 1800 K).

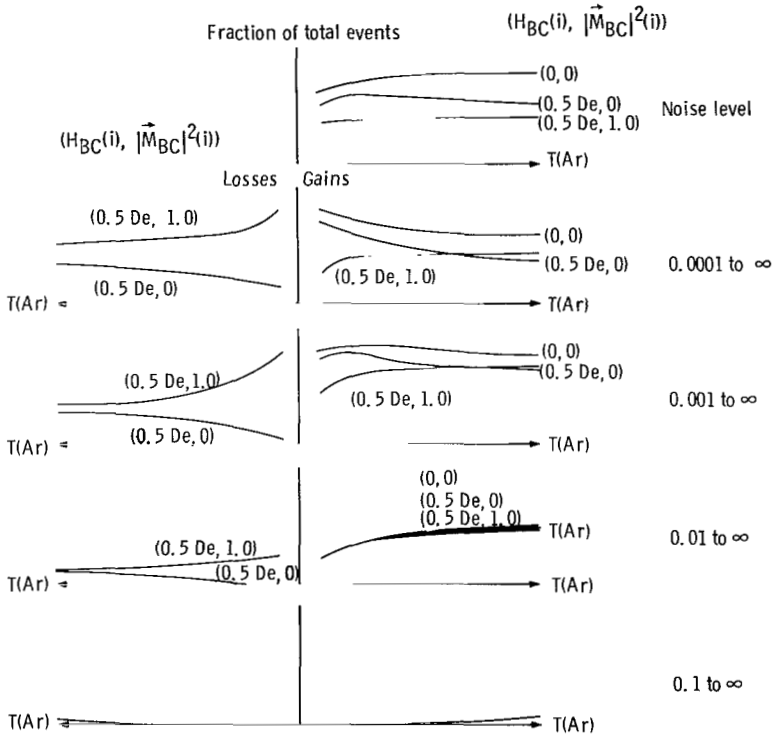

(a) Behavior of ΔH_{BC} probability distributions as function of heat bath temperature.

Figure 8. - Temperature dependence of probability distributions.

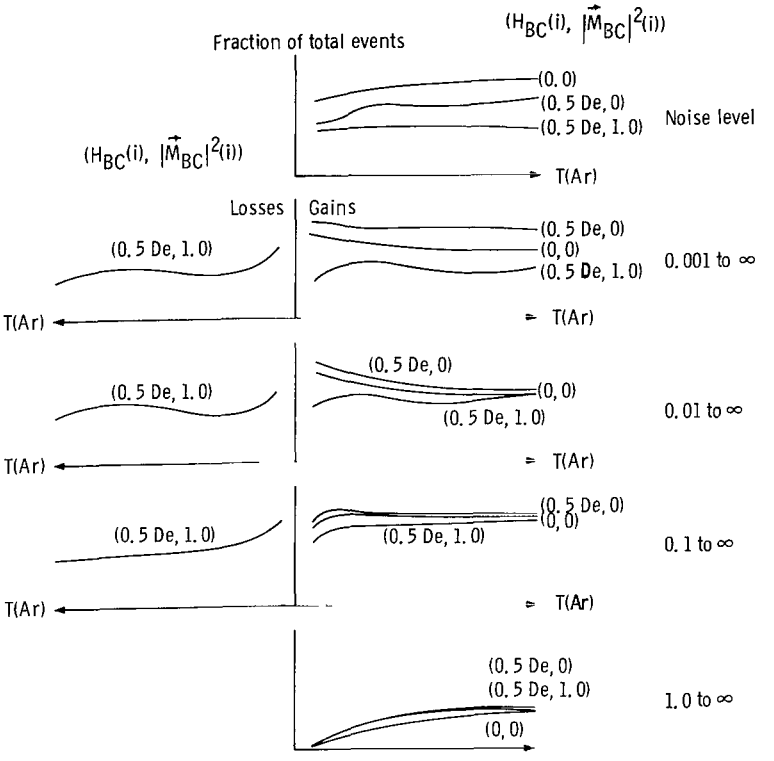

(b) Behavior of $\Delta|\vec{M}_{BC}|^2$ probability distributions as function of heat bath temperature.

Figure 8. - Concluded.

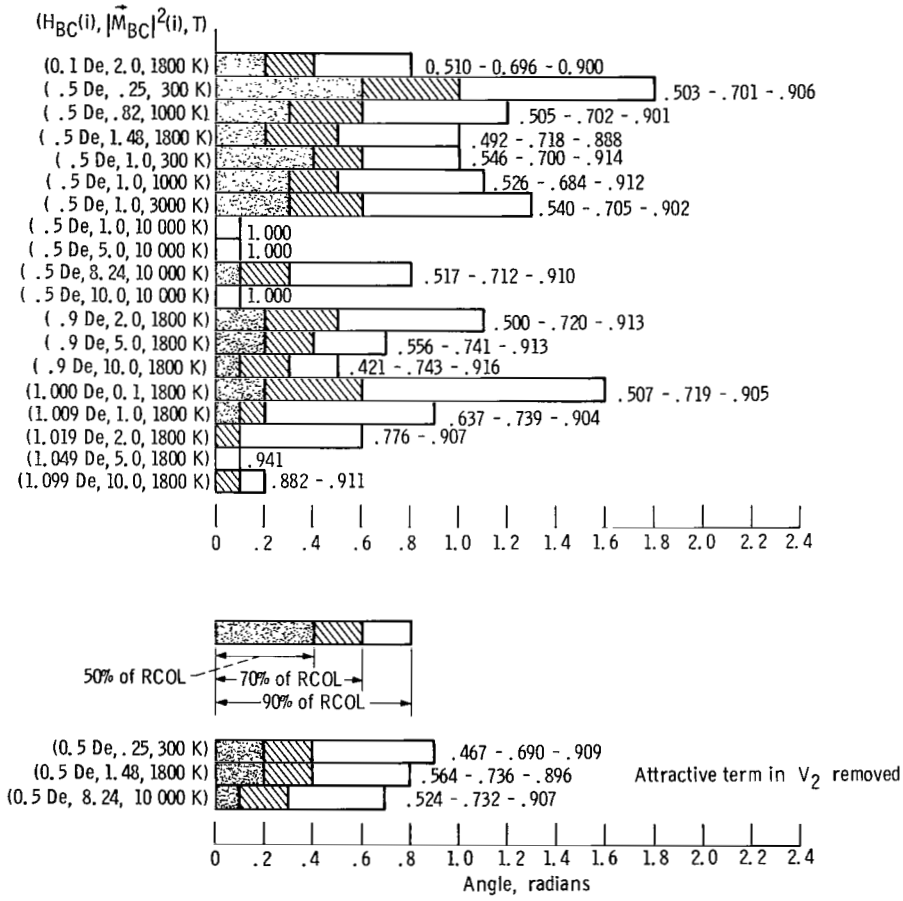

Figure 9. - Statistical tabulation of angle between $\vec{M}_{BC}(i)$ and $\vec{M}_{BC}(f)$ for several fractions of RCOL.

"The aeronautical and space activities of the United States shall be conducted so as to contribute . . . to the expansion of human knowledge of phenomena in the atmosphere and space. The Administration shall provide for the widest practicable and appropriate dissemination of information concerning its activities and the results thereof."

—NATIONAL AERONAUTICS AND SPACE ACT OF 1958

NASA SCIENTIFIC AND TECHNICAL PUBLICATIONS

TECHNICAL REPORTS: Scientific and technical information considered important, complete, and a lasting contribution to existing knowledge.

TECHNICAL NOTES: Information less broad in scope but nevertheless of importance as a contribution to existing knowledge.

TECHNICAL MEMORANDUMS: Information receiving limited distribution because of preliminary data, security classification, or other reasons.

CONTRACTOR REPORTS: Scientific and technical information generated under a NASA contract or grant and considered an important contribution to existing knowledge.

TECHNICAL TRANSLATIONS: Information published in a foreign language considered to merit NASA distribution in English.

SPECIAL PUBLICATIONS: Information derived from or of value to NASA activities. Publications include conference proceedings, monographs, data compilations, handbooks, sourcebooks, and special bibliographies.

TECHNOLOGY UTILIZATION PUBLICATIONS: Information on technology used by NASA that may be of particular interest in commercial and other non-aerospace applications. Publications include Tech Briefs, Technology Utilization Reports and Technology Surveys.

Details on the availability of these publications may be obtained from:

SCIENTIFIC AND TECHNICAL INFORMATION OFFICE

NATIONAL AERONAUTICS AND SPACE ADMINISTRATION

Washington, D.C. 20546